5. SITE 321

The Shipboard Scientific Party[1]

SITE DATA

Location: East edge of Nazca plate (Peru Basin)

Dates Occupied: 29-31 January 1974

Time on Site: 53 hours (2.21 days)

Position: 12°01.29'S; 81°54.24'W

Water Depth: 4827 meters (drill pipe)

Penetration: 134.5 meters

Number of Cores: 14

Total Length of Cored Section: 125 meters

Total Core Recovered: 85.8 meters

Percentage Core Recovery: 69%

Oldest Sediment Cored:
Depth below sea floor: 124 meters
Nature: Ferruginous nanno ooze
Age: Late Eocene
Measured velocity: 1.54 km/sec

Basement:
Depth below sea floor: 124 meters
Nature: Basalt
Velocity: 5.07-5.94 km/sec

Principal Results: The units penetrated at Site 321 are 34.5 meters of greenish-gray clay, rich in siliceous fossils, 14.5 meters of light yellow-brown clay with clear volcanic glass, 9 meters of unfossiliferous brown zeolitic clay, 66 meters of ferruginous nanno ooze, and 10.5 meters of basalt. The upper section, of late Miocene-Quaternary age, reflects the high productivity of the Humboldt (Peru) Current in its abundant siliceous fossils and the South American continent in its terrigenous clay and volcanic ash. The nanno ooze is late Oligocene-late Eocene in age, and, along with sediments of similar age at Site 320, represents the first Paleogene strata found on the Nazca plate. Faunal age corresponds well with ages based on magnetic anomalies and on the Sclater age-depth curve. The underlying extrusive basalt is massive and generally aphyric, with vesicles, calcite amygdules, and sulfide and smectite veins.

BACKGROUND AND OBJECTIVES

Geologic Setting

Site 321 is located on the eastern edge of the Nazca plate immediately south of the Mendaña Fracture Zone (Figure 1). The sea floor is 400 meters deeper than at Site 320, which lies north of the fracture zone (Figure 2). Site 321 is located about 15 km west of anomaly 16 (39 m.y. old), as recognized by Herron (1972). The half spreading rate, based on the distance from anomaly 12 to anomaly 16, is 7.9 cm/yr parallel to the Mendaña Fracture Zone.

The site is located along an ASPER refraction line at 12°S run by D. Hussong and others (personal communication, 1973) which shows low-velocity layers in the upper part of the basement. The upper basement layer has velocities of 3.1-3.8 km/sec; below this is a 5.2-5.8 km/sec, layer underlain by a 6.0-6.5 km/sec layer. About 50 km east of the site, the ASPER data suggest a thrust fault, although gravity data have not verified its existence. The sea floor rises gently east of the site prior to the more abrupt descent into the Peru-Chile Trench; this apparently results from elastic flexure of the upper lithosphere produced by loading of the Nazca plate by the leading edge of the American plate (Watts and Talwani, 1974; Ade-Hall, Underway Surveys, this volume).

Although the predicted crustal age at Site 321 is greater than at Site 320, the sediment section is thinner, possibly reflecting greater water depths and a longer time below the CCD.

The site was located from *Kana Keoki* Leg 7 (Figure 3) and lies at 2230Z, 12 January 1972, at which point the sonobuoy marking ASPER Station 104 was dropped. The surficial sediments show on the high-frequency but not on the low-frequency record, suggesting that they are quite soft. An intermediate reflector is present at a subbottom interval of 0.086 sec (2-way time).

Objectives

Objectives for drilling at Site 321 were the following: (1) to compare velocities from the basalt core with ASPER refraction data, (2) to determine the paleolatitude of the plate from remanent magnetization of basalt and of sediments, (3) to compare the magnetization of basalt at a site with and a site without linear magnetic anomalies, (4) to describe the petrology and geochemistry of the basalt, (5) to determine the history of the eastern Nazca plate for the last 40 m.y., the history of the Humboldt (Peru) Current, and the convergence of the Nazca and South American plates, (6) to compare the thinner sediment section over older crust at Site 321 with the section at Site 320, (7) to deter-

---

[1] Robert S. Yeats, Ohio University, Athens, Ohio (Co-Chief Scientist); Stanley R. Hart, Carnegie Institution of Washington, Washington, D.C. (Co-Chief Scientist); James M. Ade-Hall, Dalhousie University, Halifax, Nova Scotia; Manuel N. Bass, Carnegie Institution of Washington, Washington, D.C.; William E. Benson, National Science Foundation, Washington, D.C.; Roger A. Hart, Physical Research Laboratory, Ahmedabad, India; Patrick G. Quilty, West Australian Petroleum Party Ltd., Perth, West Australia, Harvey M. Sachs, Case Western Reserve University, Cleveland, Ohio; Matthew H. Salisbury, National Science Foundation, Washington, D.C.; T.L. Vallier, University of California at San Diego, La Jolla, California. Additional contribution by G. Blechschmidt, University of Washington, Seattle, Washington.

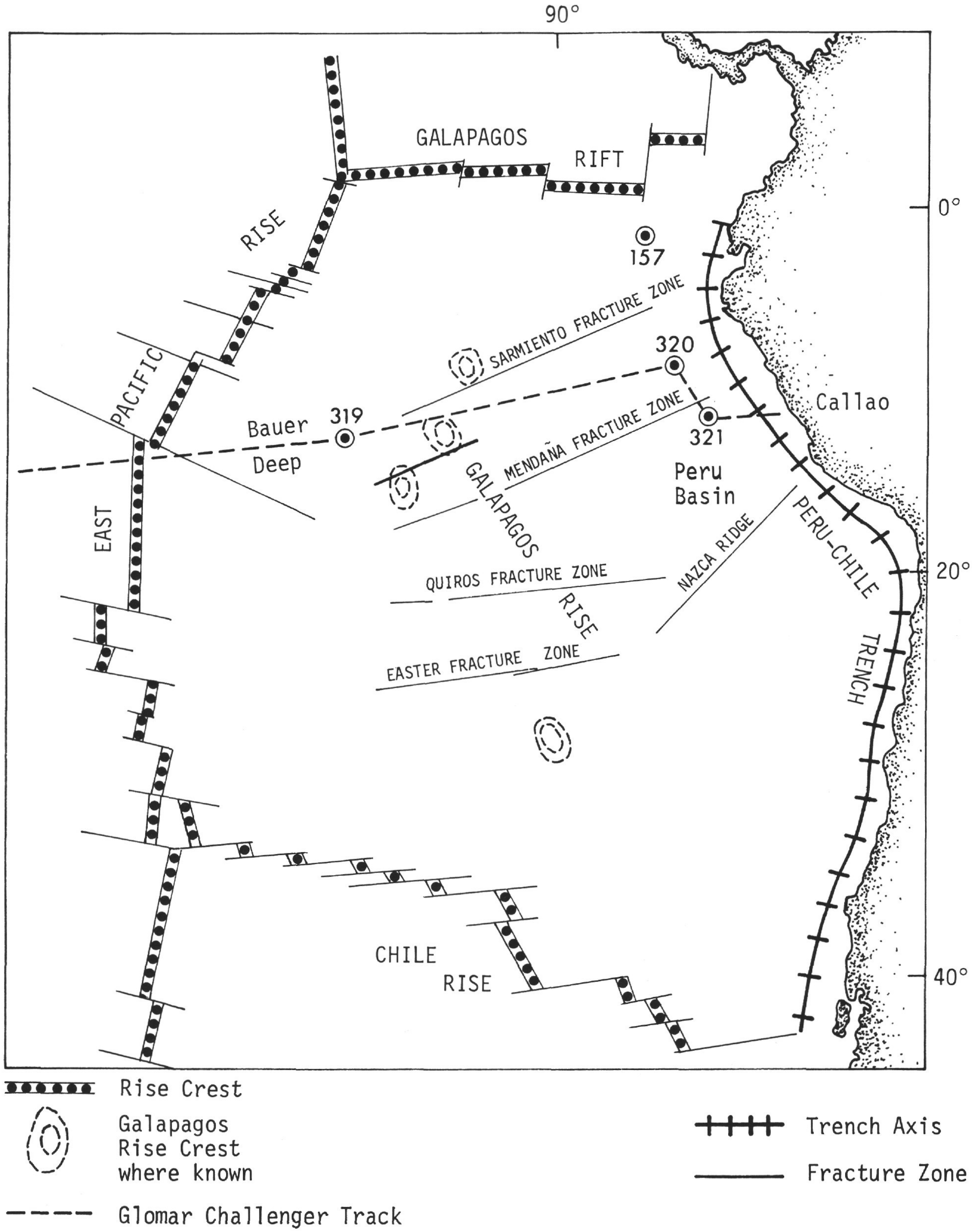

Figure 1. *Location map of sites drilled during Leg 34.*

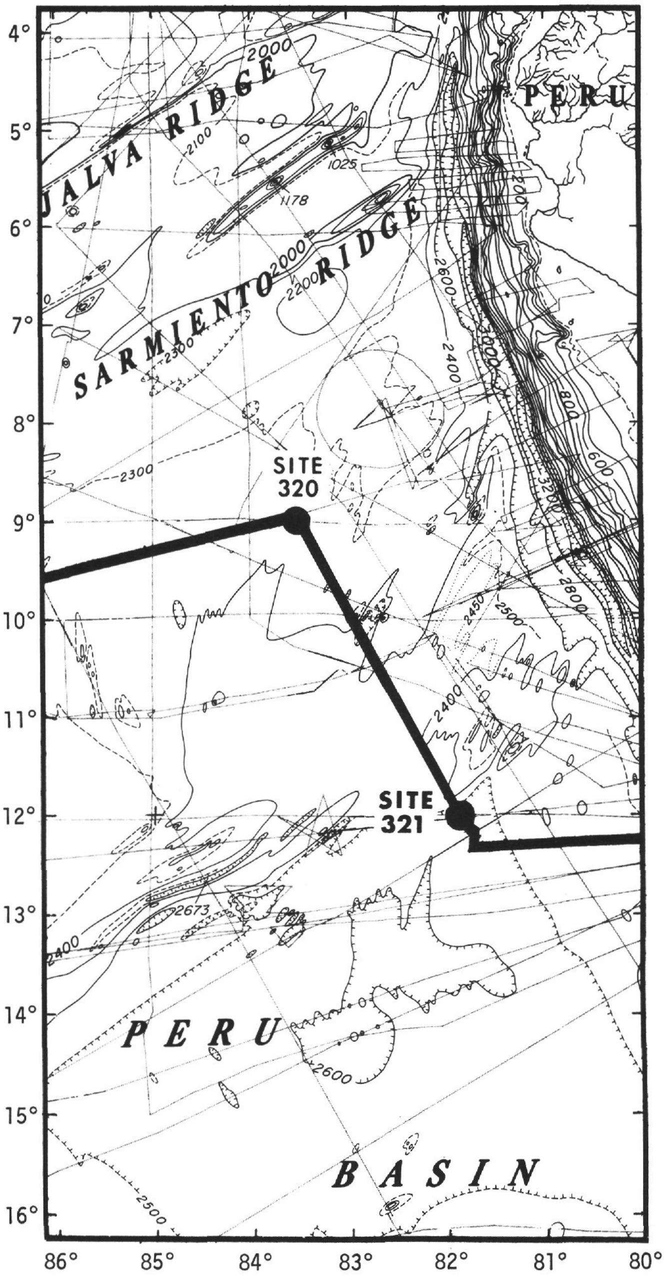

Figure 2. *Bathymetry of Sites 320 and 321 (in fathoms) from Mammerickx et al. (1975).*

mine the amount of airborne terrigenous matter in the plate, including ash from Andean volcanoes, and (8) to determine the effectiveness of the Peru-Chile Trench as a barrier to turbidity current dispersal.

OPERATIONS

Site Survey

Site 321 was located along an ASPER refraction line at 12°S run by Hawaii Institute of Geophysics as part of *Kana Keoki* Leg 7 (1971). At ASPER Sonobuoy Station 104 (2230Z, 12 January 1972 station), a small basin slightly deeper than adjacent terrain contains about 135 meters of sediment, in contrast with the 80 meters characteristic of most of the area.

Glomar Challenger approached the site from the northwest and turned east along the *Kana Keoki* track. The basin was located at a depth about 50-60 meters shallower tha on the *Kana Keoki* line. After a Williamson turn, the beacon was dropped on the run at 0745 hr (local time), 29 January as the ship steamed west over the site (Figure 4). Detailed bathymetry and ships' tracks are given in Figure 5.

Drilling Program

The program was to continuously core, leaving time for the bit to get maximum life in basalt (Table 1). The bit took weight at 4827 meters, the same depth as indicated by PDR; this depth was confirmed by the 1.5-meter core recovery. The top of the basalt was reached at 4941.5 meters, almost 1 meter above the bottom of Core 13. That core recovered basalt and sediment, but the actual contact was not preserved.

Core 14 was cut in basalt with an occasional 500 amps of torque. Weight was added and the torque decreased for the last 4-5 meters, resulting in smooth drilling and good recovery from a thick, massive cooling unit of basalt with relatively few fractures. The core barrel for Core 15 was dropped and the string worked to bottom (after being pulled above the basalt for the retrieval of Core 14). When coring began, torque rose to 750 amps, then the Kelley was rotated and torque dropped, leveling off at 150 amps. The bottom-hole assembly had twisted off above the mudline, forcing abandonment of the site.

Glomar Challenger left the site at 116 hr local time, 1 January 1974. A box survey of the site was conducted, and the ship cruised south to 12°20'S to provide magnetic anomaly correlation with *Kana Keoki* 7 and Project Magnet lines.

LITHOLOGY

Description of Units: Sediments

The hole was cored continuously to a depth of 134.5 meters with the exception of the interval from 96.5 to 106 meters. Basalt was encountered at 124 meters and was penetrated for 10.5 meters before twist off forced abandonment of the site.

The sediments are divided into four lithologic units (Table 2, Figure 6) which overlie basalt. They consist of greenish-gray, siliceous fossil-rich detrital clay (Unit 1); yellowish-brown, volcanic glass-rich clay (Unit 2); dark brown, zeolite-bearing brown clay (Unit 3); and pale brown to dark brown iron-rich nanno ooze (Unit 4).

Unit 1: Siliceous Fossil-rich Detrital Clay

The youngest unit (Core 1 through Core 5, Section 3; subbottom depth 0-34.5 m) is a greenish-gray, gray, and olive siliceous fossil-rich detrital clay of Pliocene and Quaternary age. Clay is the major component, constituting about 70% to 85% of the sediments, and siliceous fossils consist, in order of decreasing abundance, of diatoms, radiolarians, sponge spicules, and silicoflagellates, and comprise as much as 25% of some sediments in the unit. Minor components include clear volcanic glass (trace to 7%, with one sample having

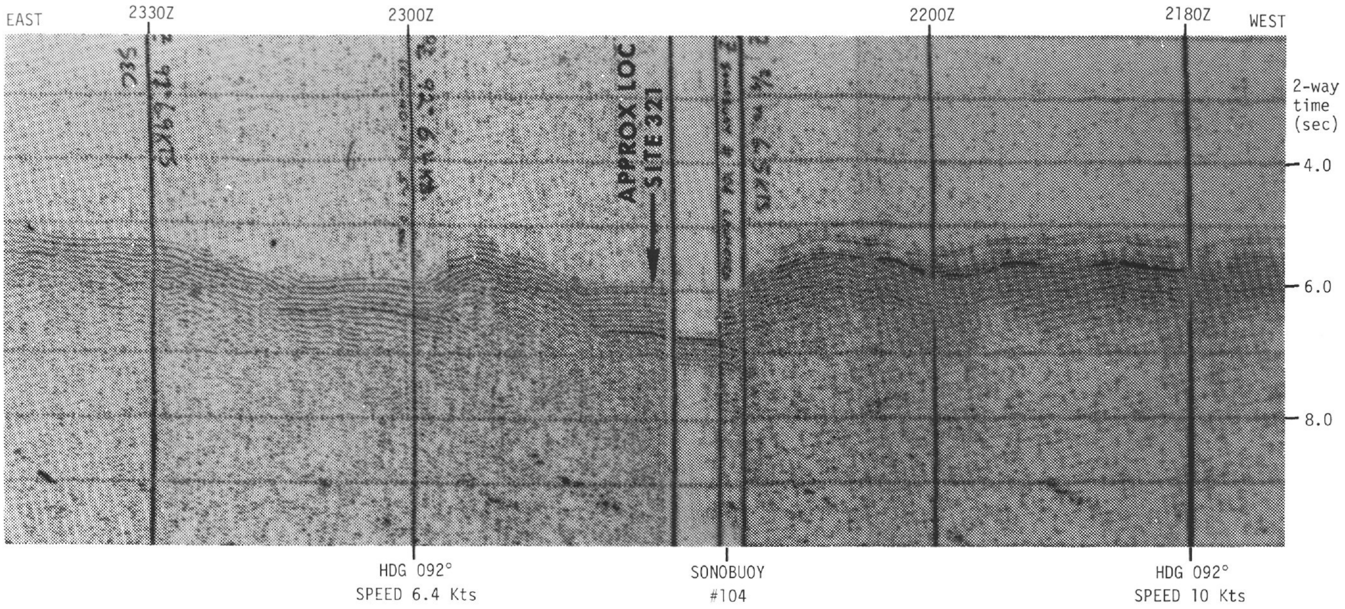

Figure 3. Kana Keoki *Leg 7 profile showing location of Site 321 at 2230Z, 12 January 1972 at point where sonobuoy marking ASPER 104 was dropped. Frequency was 40-100 Hz with a 5 sec sweep. Water depth at Site 321 is 4827 meters.*

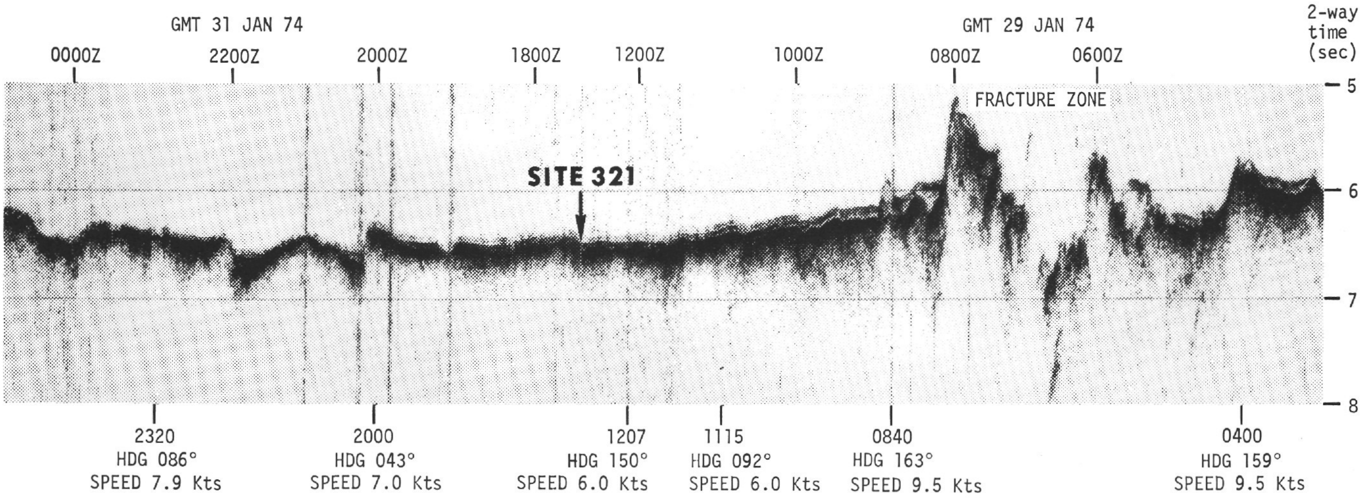

Figure 4. Glomar Challenger *airgun profile between Sites 320 and 321 and past Site 321 (10-sec sweep).*

50%), feldspar and quartz in the fine silt-size range, heavy minerals (clinopyroxene, hypersthene, biotite, and opaques), and a few fish remains. Arbitrarily, the unit can be subdivided into two subunits on the basis of siliceous fossil and volcanic glass percentages. Cores 1 through 3 have consistently higher amounts of siliceous fossils (10%-25%) and lower amounts of volcanic glass (trace to 3%), whereas Cores 4 and 5 (through Section 3) have lower siliceous fossil percentages (2%-10%) and higher amounts of volcanic glass (1%-10%, with one zone of 50%).

Unit 2: Volcanic Glass-rich Clay

The next older unit, of late Miocene and possibly younger age, is thinner than Unit 1 (Core 5, Section 3 through Core 6; 14.5 m thick) and is easily recognized by its color and lithology. The unit consists of light yellowish-brown clay near the top, below which is dark grayish-brown volcanic glass-rich clay grading downwards to clayey volcanic ash. Distinguishing characteristics are the high contents of clear volcanic glass (ranging from 5% to 55%, with an average of about 20%) and the yellow-brown and brown color. Some thin beds of grayish-green, waxy, bentonite-like material occur in Samples 5-4, 140-150 cm and 5-5, 24-30 cm. Although most of the volcanic glass is clear and fresh, some samples contain clumps and pieces of angular hard clay which suggest that they may be altered glass, and part of the montmorillonite matrix in Unit 2 probably formed by the alteration of fine volcanic ash. Some calcareous nannofossils occur at isolated intervals (e.g., Core 6, Section 3, 75 cm), and siliceous fossils are irregularly dispersed (trace to 5%). Heavy minerals include clear and green clinopyroxene, hornblende, biotite, and opaques. Euhedral crystals of phillipsite occur in the core catcher of Core 6.

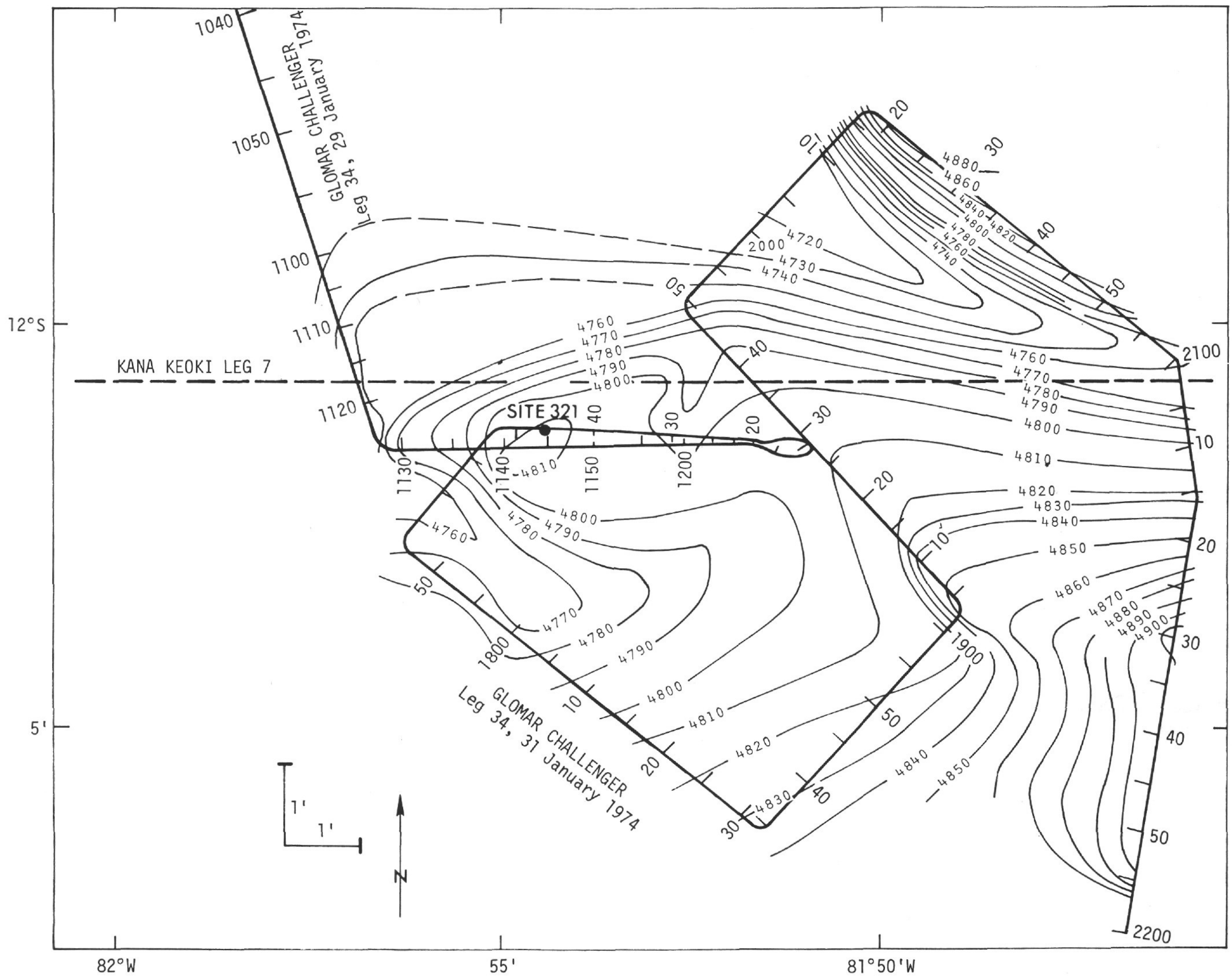

Figure 5. *Detailed bathymetry at Site 321 (in m) showing* Kana Keoki *Leg 7 and* Glomar Challenger *Leg 34 tracks. Time is in GMT.*

TABLE 1
Coring Summary, Site 321

Core	Time on Deck	Depth From Derrick Floor (m)	Depth Below Mudline (m)	Depth Below Top Basalt (m)	Recovery (m)	Recovery (%)	Remarks
1	2100 (29 Jan)	4827.0-4828.5	0-1.5		1.5	100	Took weight at 4827 (8 m water core)
2	2241	4828.5-4838.0	1.5-11.0		6.1	64	
3	0019 (30 Jan)	4838.0-4847.5	11.0-20.5		9.29	98	
4	0146	4847.5-4857.0	20.5-30.0		6.0	63	
5	0315	4857.0-4866.5	30.0-39.5		8.5	89	
6	0450	4866.5-4876.0	39.5-49.0		9.2	98	
7	0620	4876.0-4885.5	49.0-58.5		8.9	91	
8	0750	4885.5-4895.0	58.5-68.0		9.1	96	
9	0925	4895.0-4904.5	68.0-77.5		9.3	97	
10	1241	4904.5-4914.0	77.5-87.0		4.5	47	Down time; kink in sand line
11	1423	4914.0-4923.5	87.0-96.5		4.1	43	
12	1559	4933.0-4942.5	106.0-115.5		1.0	11	Core liner partly crushed in barrel
13	1806	4942.5-4952.0	115.5-125	0-1	3.8	40	Top basalt 124 meters (1 m slow drilling)
14	2225	4952.0-4961.5	125.0-134.5	1-10.5	4.5	47	500 amp torque occasionally, weight added last 4-5 meters, faster and smoother; large cooling unit, few natural fractures

TABLE 2
Lithostratigraphic Summary, Site 321

Unit	Subbottom Depth (m)	Lithology	Core	Age
1	0-34.5	Greenish-gray detrital clay, rich in siliceous fossils	1-5	Quaternary and Pliocene
2	34.5-49	Light yellow-brown clay with significant amounts of clear volcanic ash, up to 55% in a few horizons	5-6	Late Miocene and possibly younger
3	49-58	Zeolite-bearing brown clay	7	Miocene (?)
4	58-124	Light brown nanno ooze interbedded with darker brown zeolite-bearing iron-rich nanno ooze	7-13	Early Miocene to late Eocene
5	124-134.5	Basalt	13-14	(?)

Unit 3: Brown Clay

An undated zeolite-bearing brown clay unit, about 9 meters thick, was cored from 49 to 58 meters (all of Core 7 down to Section 6, 130 cm). Colors are dark brown and dark grayish-brown. Phillipsite composes from 3% to 7% of the sediment, and opaque minerals (including rare semi-opaques, the so-called RSOs) range from 2% to 5%. Trace amounts of calcareous nannofossils were noted in Sections 4 and 5; however, they may be exogenous.

Unit 4: Nanno Ooze

From 58 meters to the top of the basalt at 124 meters, the section is nanno ooze, late Eocene to early Miocene (?) in age, that has varying amounts of ferruginous grains, forams, microscopic calcite fragments, and phillipsite. The unit is yellowish-brown, pale brown, and dark brown in color. Sediment types include nanno ooze, ferruginous nanno ooze, foram-rich nanno ooze, and iron/foram/zeolite-bearing nanno ooze. High percentages of ferruginous particles (RSOs) occur in the upper part of Core 9 (10%-25%) and in Core 13 (15%-35%). Core 9 also has a high percentage of phillipsite (5%-15% in the first two sections). Phillipsite forms as much as 15% of individual samples, and euhedral cruciform twins are common. Foraminiferal tests compose a significant proportion of Cores 11 and 12, in which contents range from 2% to 20% and average about 7% in five samples. Generally, high iron and high zeolite percentages occur in the dark brown beds. Like the iron-rich sediments at Sites 319 and 320, Unit 4 at Site 321 contains only a small amount of clay. The brown colors are mainly the result of iron particles.

The basalt-sediment contact was encountered at a depth of 124 meters. Samples from directly above the contact, with high RSO and phillipsite percentages and also abundant (about 20%) particles of green altered volcanic glass (nontronite?), suggest that the contact is depositional.

Discussion of Sediments

Several points about the sediment section should be made:

1) The sediment-basalt contact is depositional. The late Eocene age of oldest sediment is that predicted from magnetic anomalies and from bathymetry. A heavy mineral separation from the oldest sediments above the basalt contains basalt-derived crystal and rock fragments.

2) The basal sediments are iron rich, apparently similar to basal sediments cored elsewhere in the world's oceans.

3) High RSO content in Core 9 (late Oligocene) is obviously not a basal iron-rich facies.

4) The contact between nanno ooze and brown clay (base of Core 7) indicates that the sea floor crossed the CCD in late Oligocene time.

5) There may be a hiatus within the brown clay unit (Unit 3), although the entire unit can be accounted for by a sedimentation rate of 1.0 m/m.y. during the early and middle Miocene.

6) Abundant volcanic products reached the site in the late Miocene (Unit 2), when clear volcanic glass became an important sediment component. These materials record the beginning of major pyroclastic activity in the Andes Mountains. High volcanic glass input has continued to the present time.

7) Although siliceous fossils are not abundant in Unit 2, their appearance may mark the beginning of increased productivity, either because of the initiation of the Humboldt (Peru) Current or because the site moved under the influence of that current for the first time in the late Miocene.

8) The top unit is marked by large quantities of green detrital clay and siliceous fossils. The high clay content is related to the site's proximity to the South American continent, whereas the siliceous fossils are related to the high biologic productivity associated with the cold, nutrient-rich waters of the Humboldt (Peru) Current.

9) In summary, major events which affected the sediment column at Site 321 occurred: (a) in the late Eocene-early Oligocene, when high contents of iron oxide were deposited; (b) in the early late Oligocene, when once again ferruginous particles formed a significant portion of the sediment; (c) in latest Oligocene, when the sea floor subsided below the CCD; (d) in the late Miocene when abundant pyroclastic materials reached the site; and (e) in the Pliocene-Quaternary, when siliceous fossils and detrital clays were deposited.

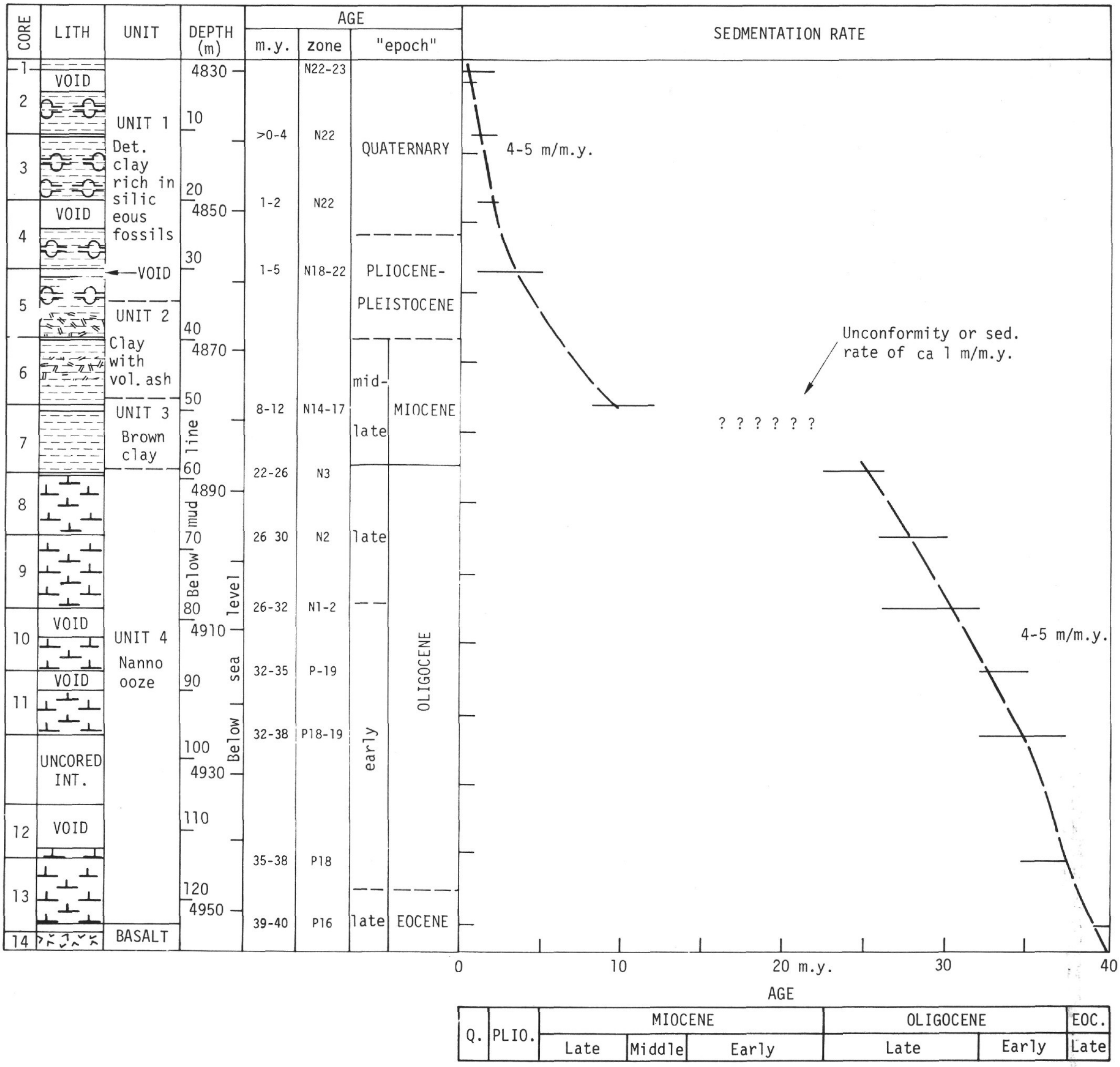

Figure 6. *Stratigraphic column at Site 321, showing age data and sedimentation rates. Horizontal lines on sedimentation rate diagram show precision.*

Description of Units: Basalt

Basalt was recovered in the lowest 25 cm of Core 13 and in Core 14 with about 50% recovery. The rock is remarkably uniform from top to bottom of the recovered section, varying from fine-grained, massive, dark gray, almost aphyric basalt at the top, to very coarse grained but otherwise identical basalt at the bottom. No glass was recovered except for one angular fragment of dark brown glass in the +63 micron fraction of a slurry from the liner of Core 14. Grain size variations indicate two cooling units with a contact at Core 13, Section 4, 125 cm. The basalt-sediment contact is disturbed; the top 15 cm is a half cylinder bounded by the surface of the core and a steep to vertical joint, and it almost certainly would not have survived coring had the other half of the cylinder originally been sediment. The other half of the basalt cylinder must have been lost during coring. Nonetheless, the basal sediment is rich in basaltic minerals and altered palagonite and fibropalagonite and undoubtedly was originally deposited near the contact. Therefore, either the original contact was lost in coring, or it had been previously eroded.

The lower, thicker cooling unit is homogeneous. Although neither contact was recovered, the fine grain size of the uppermost pieces recovered indicates proximity to the upper contact, and the decrease of frequency and continuity of joints and veins near the bottom of the recovered core may indicate proximity to the lower contact. Most of Core 14 is composed of nonrotated core pieces that can be refitted into an almost continuously recovered section, from which we infer that the lost 50% of the drilled section was the lower half of the core, which may have been a relatively nonjointed, coarse-grained portion of the thicker cooling unit which for some reason was not retained in the core barrel, or a pillowed, finely jointed section below that unit which was destroyed by the bit as in Hole 320B.

Microphenocrysts are rare. Plagioclase is most abundant and ranges in size from 0.4 × 0.1 mm to 3 × 0.2 mm, with maximum dimensions rarely exceeding 2 mm. The cores of plagioclase microphenocrysts from Core 14, Section 4, 34-49 cm are An_{65-72}. Olivine microphenocrysts are very rare; one from the thin, upper cooling unit is Fo_{87-88}. A clinopyroxene microphenocryst was seen only as a component of a glomerocryst. The plagioclase and olivine compositions suggest normal, ridge-type olivine tholeiites. An interval from 14-2, 45 cm to 14-4, 2 cm is totally devoid of microphenocrysts and suggests the existence of a complementary cumulate zone below the recovered section. In a general way, the abundance of microphenocrysts increases in finer grained rocks near inferred contacts of cooling units, and such abundance variations in microphenocryst-poor rocks may offer one criterion for proximity to contacts.

Textures are intergranular, verging on subophitic. The groundmass contains sector zoned pyroxene with wavy extinction, plagioclase microlites, opaque minerals, and smectite pseudomorphs after late olivine. In the coarser grained rocks the last-crystallized, quenched mesostasis includes elongate, skeletal opaque minerals and skeletal plagioclase in a smectite (altered glass?) matrix. This terminal quench is similar to that inferred from the coarse-grained rocks from Site 319 and similarly suggests a flow rather than a sill. The presence of groundmass olivine indicates that the magma lay on the olivine-plagioclase cotectic or the olivine-plagioclase-augite three-phase cotectic throughout the course of crystallization. Thus, as expected in such fine-grained rocks, fractionation was not pronounced.

High titanium titanomagnetite is the dominant opaque phase in all 12 basalt samples examined. Grain form varies from skeletal to anhedral or subhedral. Grain size varies from the limit of visibility at about $1/4\mu$, in the finer grained basalts of Core 13, to 30μ in the massive basalts of Core 14. Two size generations are often evident in the massive basalts, with the finer size generation grains often forming overgrowth rims on the larger skeletal to anhedral grains. Titanomagnetite alteration is limited to the low-temperature effects resulting from the halmyrolysis of the lavas, which produces cation-deficient titanomagnetites, and leads ultimately to the formation of titanomaghemites. The development of cation deficiency can be followed by changes in magnetic properties (see Ade-Hall et al., Rock Magnetism of Basalts, Leg 34, this volume). In turn, changes in titanomagnetite detected with the ore microscope can be assigned arbitrary numerical values of cation deficiency on a scale from 0.0 to 1.0 calibrated by the magnetic measurements. Low degrees of cation deficiency are identified by the presence of volume change cracks in otherwise apparently unaltered grains. Cation deficiencies in excess of 0.6 are identified by lightening in color, increased reflectivity and expulsion of iron into surrounding silicates. The degree of cation deficiency of titanomagnetite correlates with the type of basalt, the titanomagnetites in the fine-grained basalts being highly cation deficient, and those in the massive basalts being little if at all cation deficient.

Natural fractures of joints (inferred from vein distribution) are low dipping near the top and steeply inclined in the lower portion of the recovered section. The low-dipping joints appear to form preferentially in fine-grained rocks near contacts of cooling units, the steeply inclined ones in coarser grained rocks from the interiors. The continuity of joints decreases and their spacing increases downward, and these changes correlate with improved core recovery.

Veins include green and blue-green unoxidized smectite in the lower, relatively fresh, sparsely jointed part of the recovered section; and red, brown, and yellow oxidized smectites in the higher, relatively altered, jointed and veined portions nearer the contacts of the cooling units. Sulfide and phillipsite occur with some of the unoxidized smectite, and sulfide is locally the dominant vein mineral. The light grayish or whitish-yellow color of much of the sulfide gave a shipboard clue to the presence of marcasite, later confirmed by X-ray diffraction analysis, which occurs with pyrite in veins in basalt from Site 321 as well as Site 319. As at Site 319, detailed textural relationships of the variously colored smectites suggest an earlier, nonoxidative stage of alteration and a later oxidative one. Calcite is commonly a minor component of veins and less commonly the dominant mineral. Overall, it is much less abundant than in veins from Site 319. Aragonite, despite optical suggestions of its presence during shipboard examination, was not confirmed by X-ray diffraction analysis. If ever present, as at Site 319, it totally inverted to calcite during the additional 15 m.y. of time available at Site 321.

Vesicles appear throughout, constituting about 1% of the rock. Maximum diameters increase from less than 1 mm near the top of the recovered section to 2 mm near the bottom; diameters are generally 0.7 mm or smaller. They commonly contain quenched, very fine grained basalt in their bottoms. Locally the vesicles coalesce to irregular holes up to 4 mm across. The vesicles are commonly empty or thinly lined by oxidized smectite in the altered rocks. In the fresher, grayer rocks there is a greater tendency to partial or complete fillings (i.e., amygdules) which are commonly smectite or sulfide near smectite or sulfide veins, respectively. Below 321-14-1, 55 cm, many vesicles are partly to wholly filled by calcite, often radial, which may enclose a sulfide grain or be rimmed by green smectite. Many empty or thinly lined vesicles are evidently artifacts of drilling and sawing due to the tendency of smectite to swell and pluck out, especially in fresh water. In the lower part of Core

14 the carbonate-filled vesicles decrease rapidly in abundance parallel to a notable decrease in frequency and continuity of joints and veins of all types.

BIOSTRATIGRAPHY

Neogene opaline microfossils are the dominant fossils above 58 meters (just above 321-7, CC), and planktonic foraminifera apparently are totally absent above 58 meters, although a few agglutinated forms are present in the core-catcher samples of Core 4 (30 m). Below 58 meters, the sediments are dominantly nanno oozes, Oligocene-Eocene in age, with abundant planktonic foraminifera. Biostratigraphic information is summarized in Figure 3.

Neogene Radiolarian Stratigraphy

Neogene Radiolaria were recovered only from the upper part of Site 321. Core catchers 1-3 (0-20.5 m) contain well-preserved Quaternary faunas; core catcher 4 (30 m) has a Pliocene or Quaternary assemblage; core catcher 5 (39.5 m) contains a sparse assemblage lacking stratigraphically useful forms; core catcher 6 (49 m) contains a very sparse earliest late Miocene (lower part) fauna; and core catchers 7 (58.5 m) to 13 (124 m) contain virtually no Radiolaria. In addition to Radiolaria, there are numerous well-preserved diatoms and silicoflagellates in core catchers 1-3.

Core catchers 1-3 contain diverse and well-preserved radiolarian faunas which resemble those of the Panama Basin and Equatorial Pacific. The assemblage of core catcher 1 contains *Pterocanium praetextum, Ommatartus tetrathalamus,* and *Theoconus minythorax.* The *Amphirhopalum ypsilon* generally shows about five chambers on the forked arm before bifurcation. This tends to put this sample in the uppermost Quaternary Zone, but the dominant form, *Buccinosphaera invaginata* was not encountered. The absence of *Stylatractus universus* probably indicates that core catcher 1 sediment is less than about 400,000 yr old, if the North Pacific disappearance datum represents extinction.

Core catchers 2 and 3 contain assemblages as rich as that of core catcher 1, and also increasingly abundant *Stylatractus universus,* indicating an age greater than about 400,000 yr. In both, the *Amphirhopalum ypsilon* tends to have only two chambers on the forked arm before bifurcation, indicating earlier Quaternary ages. Core catcher 3 is considered to be Quaternary because *Pterocanium prismatium* was not found, despite the abundance of other *Pterocanium* species. It is noteworthy that neither *Spongaster pentas* (lower Pliocene) nor *S. tetras* was encountered at Site 321.

Core catcher 4, from an ash-rich zone, contains a rather sparse fauna with post-Miocene affinities. *Ommatartus tetrathalamus, Stylatractus universus,* and *Lamprocyclas maritalis* are present. The "*Amphirhopalum*" present have three completely separate arms. In the absence of any *Pterocanium* or either *Spongaster pentas* or *S. tetras,* discrimination between Pliocene and Quaternary was not feasible.

Core catcher 5 is nearly barren, with rare robust stylatractoids including one *Stylatractus universus.* Because the range of this form extends into the late Miocene, its presence offers little significant stratigraphic information.

Core catcher 6 contains a sparse fauna with most forms broken. Cannartids are dominant, but end caps are almost never preserved. Positive identification of *Ommatartus hughesi* from several partial samples and a complete end cap strongly indicate that the fauna belongs to the *Ommatartus antepenultimus* Zone, of earliest late Miocene age.

Paleogene Planktonic Foraminiferal Stratigraphy

The nanno ooze section (58-124 m; Cores 7-12) contains a virtually complete Oligocene (P18-N3) section and the sample examined from Core 13 (124 m) is Eocene (P16) in age. There is a gap in the sequence between 96.5 and 115.5 meters.

In Core 7 (core-catcher sample) the fauna consists of very few species, those remaining are the survivors of quite obvious dissolution effects. The fauna consists mainly of benthonic foraminifera and a concentrate of fish teeth and bone fragments. Significant planktonic species are *Globigerina prasaepis, G. venezuelana, Catapsydrax unicava unicava,* and *C. dissimilis ciperoensis.*

The fauna in Core 8 consists only of small species of planktonic foraminifera showing no signs whatsoever of dissolution. No large species such as these characterizing the 7, CC sample are present. Dominant forms are species of *Chiloguembelina,* and also present are *Cassigerinella chipolensis* and *Catapsydrax stainforthi praestainforthi.*

The Core 9 sample consists of a concentrate of fish fragments resulting from marked carbonate dissolution. Characteristic planktonic foraminifera are *Globigerina prasaepis, G. sellii, Globorotalia opima nana,* and *Catapsydrax unicava unicava* of the Oligocene (P19).

Core 10 is of early Oligocene age (P18). Foraminifera again suffer the effects of dissolution but not as markedly as in some samples above. Characteristic species are *Globigerina angiporoides minima, G. prasaepis, G. winkleri,* and *?G. tapuriensis.*

The fauna in Core 11, of early Oligocene age (P18) consists of very abundant diverse foraminifera showing no dissolution effects. Characteristic forms are *Globigerina prasaepis, G. tapuriensis, G. ampliapertura, G. angiporoides, Globigerinita unicava unicava,* and rare *Chiloguembelina* species.

Again, the fauna is very rich in Core 12 (early Oligocene, P18), and makes up the largest proportion of the ooze of any samples from this hole. The fauna is unusual in being very much dominated by *Chiloguembelina* species (more than 30% of the fauna) and *Cassigerinella chipolensis. G. eocaena* also is present. *Pseudohastigerina naguewichiensis* and *Globigerina tapuriensis* are the other key fossils.

The sample from Core 13 is within about 30 cm of the basalt contact, and is the oldest sediment identified on the Nazca plate and represents the only Eocene from Leg 34. Dissolution effects are very marked, and the fauna is a rich concentrate of fish teeth and fragments. *Hantkenina* spines are common but no complete specimens were recovered. *Cribrohantkenina inflata* is identified on the basis of a single apertural face and spine. Other key species are *Globigerapsis index, G. mexicana* (*G. semiinvoluta*), and *Pseudohastigerina micra*.

The sediments above 58 meters represent sedimentation below the CCD as no calcareous microfossils (apart from rare nannoplankton) are present, and there is no evidence that they were ever present. The nanno ooze below 58 meters probably was deposited near the CCD as some faunas show dissolution effects but others show none. During the Eocene-Oligocene time interval, the CCD probably fluctuated enough to account for the variation in preservation that is seen.

Calcareous Nannoplankton

For the most part, Cores 1 through 6 are barren of calcareous nannofossils. Occasional badly corroded placoliths are present in some samples, but these are not age diagnostic. Sections 1 through 5 of Core 7 are also barren of calcareous nannofossils, but Section 6 contains a well-preserved and fairly diverse nannofossil assemblage of early Miocene-late Oligocene age. A reasonably complete late and middle Oligocene section is present in Cores 7 through 11. Precise zonal determinations are difficult due to reworking of early Oligocene and late Eocene taxa, which form a minor component of all assemblages found. Cores 8 and 9 are late Oligocene in age and are tentatively assigned to the *Sphenolithus distentus-Sphenolithus ciperoensis* zones (NP24-25). Cores 10 and 11 contain middle Oligocene nannofossils, probably representing the *Sphenolithus predistentus* Zone (NP23). The lowermost Oligocene is either missing at this site or has been lost in coring. Core 13 is late Eocene containing common *Discoaster barbadiensis* and *Discoaster saipanensis*.

SEDIMENTATION RATES

The Oligocene-Eocene sediments at Site 321 (Cores 7-13 inclusive; 58-124 m) accumulated at 4.0-5.0 m/m.y. (Figure 6). The Miocene (early part of the late Miocene) and younger sediments at Site 321 also yield a sedimentation rate of 4.0-5.0 m/m.y. although this is an average value and it actually may be lower in the Miocene and higher in the Pliocene-Quaternary.

No middle Miocene has been identified from Site 321, and the lithologic change at 58 meters from nanno ooze with abundant planktonic foraminifera upward, to zeolite-bearing brown clay may include either an unconformity of about 12 m.y. or there may be an interval of very slow sedimentation at a rate less than 1.0 m/m.y.

Although no diagnostic fossils were found in the zeolitic clay at Site 321, dating of sediments immediately above and below indicates that this unit accumulated from about 24 to 10 m.y. ago. The unit is nine meters thick, so its average sedimentation rate is very low, about 0.6 m/m.y. If sediment like that above or below the zeolitic unit had accumulated instead, with an average accumulation rate of about 3.0 m/m.y., the section would have been about 45 meters thick instead of 9 meters. It is interesting to note that this difference is approximately the difference in total sediment thickness at Sites 320 and 321. More importantly, the sedimentation rate observed, the reduction from the "expected" sediment thickness, and the lithology of the unit all indicate that the zeolitic clay represents more-or-less continuous accumulation beneath the CCD without abnormally high terrigenous influx.

The figures given here indicate a low organic productivity rate throughout all of the Cenozoic, except the Pleistocene-Holocene (Kulm et al., this volume).

GEOCHEMICAL MEASUREMENTS

Six fairly equally spaced "mini-core" samples were taken at subbottom depths ranging from 6.0 meters to 118.5 meters in the 124 meters of sediment. *p*H values for this site should be considered qualitative rather than quantitative. Measurement problems occurred with both electrodes and, for one depth (24.5 m), they gave *p*H values varying by 0.8 *p*H units. The combination electrode gave a surface seawater *p*H of 8.17. In the sediments it began at 7.65 (at 6.0 m), rising to 8.23 (at 24.4 m) then dropping at 7.45 (at 45.4 m) and gradually increasing to 7.50 at the lowest sample depth. The punch-in electrode gave a similar surface seawater *p*H of 8.11, but started much lower in the sediments at 7.09 (at 6.0 m). The trend paralleled that of the combination electrode, but the readings were lower.

Alkalinity values from potentiometric titration of the six samples varied irregularly down the length of the sedimentary column and the results from the less accurate colorimetric indicator method verify this trend. Surface seawater alkalinity was determined to be 2.39 meq/kg.

Surface seawater salinity was measured at 35.5^0/oo. The interstitial water salinities are 34.9^0/oo in the surface sediments, rising to 35.2^0/oo at 24.4 meters and remaining at that value throughout the rest of the sedimentary column.

Ten analyses of H_2O (released above 35°C) and CO_2 were made on Site 321 basalts and are summarized in Table 3. High values of CO_2 reflect high concentrations of calcite-filled amygdules in Site 321 basalts. The single H_2O value measured on the uppermost basalt core (at the bottom of the thin, upper cooling unit) is significantly higher than those on the massive section recovered in Core 14. The uppermost section is similar to the more altered sections of Site 320 in H_2O content, while the massive underlying unit has very similar H_2O values to the massive unit cored at Hole 319A, and these relations are consistent with the expectation from lithologic comparison.

TABLE 3
H_2O and CO_2 Contents of Site 321 Basalts

Sample (Interval in cm)	CO_2 (%)	H_2O Total (%)
13-4, 119-124	0.14	1.64
14-1, 42-45	0.28	0.63
14-1, 99-102	0.42	1.22
14-2, 9-12	1.19	0.78
14-2, 127-130	0.36	1.27
14-3, 7-10	0.38	1.46
14-3, 93-96	1.20	1.22
14-4, 7-10	0.24	1.39
14-4, 61-66	0.30	1.32

PHYSICAL PROPERTIES

Wet-bulk density, porosity, sonic velocity, acoustic impedance, thermal conductivity, and magnetic property determinations were made throughout the sediments. These measurements, with the exception of thermal conductivity and the addition of electrical resistivity, were continued in the underlying basalt. The results of these determinations are presented with the core descriptions.

The upper 58 meters of sediment displays a slight increase in sonic velocity (1.52 to 1.54 km/sec) downward, while wet-bulk density and thermal conductivity remain almost constant (1.30 ±0.16 g/cc and 1.83 ±0.12 mcal/cm sec°C, respectively), reflecting an almost constant porosity (4 ±7%).

Below 58 meters the porosity decreases abruptly to 60%, a value maintained with little variation (±7%) throughout the rest of the sediment column. Concomitantly, wet-bulk density rises abruptly to a relatively constant value of 1.70 ±0.08 g/cc, whereas sonic velocity and thermal conductivity values rise slowly (and in the instance of sonic velocity, erratically) over the same interval, with values ranging, respectively, from 1.51 to 1.57 km/sec and 2.08 to 3.09 mcal/cm sec°C.

It was observed for Site 319 and 320 sediments that most sediment properties are strongly porosity dependent. It is particularly clear at this site that porosity is strongly lithology dependent, the clays having much higher porosities than oozes, due to absorbed water.

As can be seen in Figure 7, the basalt bulk densities in the upper, thin cooling unit, adjacent to the sediment-water interface, are quite low, ranging from 2.72 to 2.86 in the uppermost meter. Below this level, however, densities abruptly increase to approximately 2.92 g/cc, a value maintained with very little variation (±0.04 g/cc) throughout the rest of the cored basement interval. Though the degree of alteration in the topmost meter is consistent with the age of the site, the shallow penetration of oxidative weathering was unexpected, and is probably due to the relatively unfractured, impermeable nature of the thick lower unit. Seismic velocities of basalt are density dependent, and densities may be greatly reduced by progressive submarine weathering. Local variations in weathering due to the massive versus fractured nature of the basalt, which is so well illustrated by the basalts from Sites 321 and 319, may be responsi ble for much of the great variability in velocities observed for crustal layer 2.

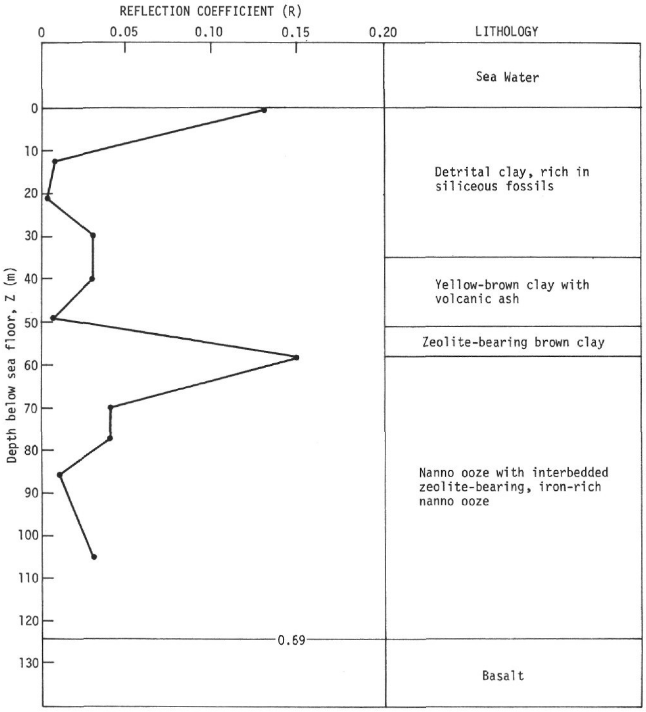

Figure 7. *Reflection coefficients* (R) *versus depth and lithology below the sea floor, Site 321.*

Sonic velocities measured using the Hamilton frame (P_h=0) are very low (5.07 km/sec) in the uppermost meter, and rise to an average of 5.8 km/sec ±0.2 km/sec at greater depths.

MAGNETIZATION OF THE BASALTS AND SEDIMENTS

Shipboard and shore-based paleomagnetic measurements on the basalts recovered at this site suggest that at least three time units were penetrated. After alternating field remanence cleaning, original magnetizing field inclinations for these units of +22, -22, and -16 ±2° were obtained. These inclinations are closely grouped around the dipole field inclination for the present latitude of the site of 23°. The agreement of the paleomagnetic and present inclinations for the site indicates that negligible net latitudinal absolute plate motion has taken place during the last 40 m.y. Paleomagnetic inclinations for the basal part of the sediment column overlying the basalts also average close to the dipole field inclination, supporting the interpretation of the basalt paleomagnetic results.

The massive basalts for Core 14 have large soft component contributions to their NRMs. These have shallow downward inclination and presumably largely represent the present earth's field at the site. NRM analysis, together with anhysteritic magnetization experiments, show that the soft and hard components are in opposition for the unit with cleaned NRM inclination of -16°. Original magnetization during a reversed polarity epoch is implied by this opposition of hard and soft components.

NRM intensity varies by two orders of magnitude from 3.9×10^{-4} to 333×10^{-4} emu cm^{-3}, with the massive basalt of Core 14 being most strongly magnetized. Induced magnetization contributes negligibly to the overall magnetization of the basalts.

Variation of NRM intensity, initial susceptibility, and saturation magnetization is largely controlled by the degree of cation deficiency of titanomagnetite, the magnetic phase of the basalts (see Ade-Hall et al., Rock Magnetism of Basalts, Leg 34, this volume). The degree of cation deficiency ranges from 0.00 to 0.79 on a 0 to 1 scale. Stoichiometric titanomagnetite occurs only in a few massive basalt samples and has a composition of $0.63Fe_2TiO_4 0.37Fe_3O_4$. Mild cation deficiency characterizes the titanomagnetite of other massive basalts while a high degree of cation deficiency is typical of the oxide phases in the fine-grained basalts of Core 13. The three magnetic properties listed above all decrease sharply with increasing cation deficiency. Thus, the halmyrolysis history of the basalts, which is responsible for cation deficiency in the titanomagnetite, has determined the magnetic state of the basement sequence drilled at this site.

CORRELATION OF REFLECTION PROFILE WITH DRILLING RESULTS

The airgun survey of the site suggests the presence of a thin (0.134 sec total 2-way travel time), but relatively complex sediment cover with two strong reflectors, the deeper of which reflects very strongly and separates the sediments from the basement.

As at Site 319, a marked discrepancy (0.022 sec) between PDR and airgun reflection times from the sea floor suggests the presence of a thin surficial sediment layer which is acoustically transparent at airgun frequencies. The 2-way travel times presented in Table 4 are thus increased by this amount to get the final values.

Correlation of the reflection profile (Figure 7) with both the drilling record and the physical properties data are straightforward. If the intracore reflectivity coefficients are computed from measured velocities and densities and plotted as a function of depth below the sea floor, a strong reflector is anticipated at 58 meters. This reflector lies at the estimated depth of the 0.086-sec reflector and thus clearly marks the major lithologic boundary between the two major units at this site, namely, that between the Miocene through Quaternary clays in the upper part of the column and the Eocene through Oligocene nanno ooze in the lower part of the column. It is interesting to note in the context of sea-floor spreading, that a lithologic change of the same type is responsible for the only major reflector seen at Site 319, in which instance its age is upper Miocene. It should also be noted that the strength of this reflector at Site 321 is due to the comparatively short depth interval over which the clay-ooze transition occurs. The absence of a lithologic transition zone is due to the presence of an unconformity at this site in the early Miocene.

The weak reflector seen in Figure 7 at 0.042 sec probably corresponds to the slight increase in reflectivity at approximately 35 meters caused by a change from clay with siliceous fossils to clay with volcanic glass. The zeolite-bearing clay unit between 49 and 58 meters depth is apparently too thin to be detected. The strong basal reflector, of course, represents the sediment-basalt contact.

TABLE 4
Reflection Intervals From PDR and Airgun Surveys, Site 321

Subbottom 2-way Time Interval	Character of Reflector	Evidence
0-0.042	Weak	PDR, drill recovery, airgun
0.042-0.086	Strong	Airgun
0.086-0.156	Strong	Airgun

As for Sites 319 and 320, the mean sediment velocity computed from the drilled sediment thickness and observed travel times is in excellent agreement with measured Hamilton frame velocities, despite core disturbance.

SUMMARY AND CONCLUSIONS

Site Survey

In addition to the *Glomar Challenger* survey conducted on the approach to Site 321, an extensive survey was conducted on departure. The topographic relief in the immediate vicinity of the site is low. Below the surface, a nearly transparent, faintly layered unit (siliceous-fossil and zeolitic clays) overlies a more strongly reflecting layer (ferruginous nanno ooze) which in turn rests unconformably on basaltic basement of moderate relief. North of the site is a fairly steep, east-trending scarp. The general topography within several kilometers of the site suggests block-faulted basement with faults trending east to southeast (see Figure 4). These are not obviously correlated to major tectonic features.

Between Site 320 and Site 321, *Glomar Challenger* crossed the Mendaña Fracture Zone, a broad, northeast-trending belt of faulted basement blocks which locally rise above and locally sink below the general level of the terrain. These blocks are mantled with sediment, and sediment thicknesses on the high-standing blocks are significantly less than at Site 321. The strong reflector at the top of the nanno ooze may be tracd north into the Mendaña Fracture Zone where, at two places, (0230Z and 0900Z, 29 January, 1974) the nanno ooze appears to be overlain with angular unconformity by the siliceous-fossil clay (Figure 4).

Sediments

The uppermost 34.5 meters of sediment consist of greenish-gray detrital clay, rich in siliceous fossils which indicate a Quaternary and Pliocene age. The presence of green clay suggests a terrigenous origin, presumably from South America. The absence of coarse-grained sediments, for example turbidites, such as those found in the continental margin of Peru, indicates that the Peru-Chile Trench has been an effective barrier to sediments transported by bottom currents, and suggests that the clays may have reached the site by nepheloid layer transport. Minor amounts of clear volcanic glass are present, most abundantly near the base of the unit. No calcareous fossils were found, and the sediments were presumably deposited below the CCD.

The next lower unit consists of 14.5 meters of light yellow-brown clay with 0.5% to 55% clear volcanic glass. Most of the clay is smectite derived from the alteration of volcanic sediments. Siliceous fossils are much less common than above and indicate a late Miocene age. This clay is underlain by 10 meters of zeolite-bearing brown clay which is unfossiliferous except for trace amounts of nannofossils.

The sedimentation rates in the younger sediments are high (especially the top 35 m) and may be due to the large percentage of siliceous fossils and to an increase in terrigenous input from the South American continent (Kulm et al., this volume). This may reflect higher biologic productivity due to the influence of the nearby, strong, north-flowing Humboldt (Peru) Current. It is possible at this site to distinguish between Humboldt (Peru) Current influences (higher biologic productivity, cooler water fauna) and continental influences (higher clay and/or volcanic ash content). The larger amount of volcanic glass in the Miocene, when presumably, the site was farther from South America than in the Pliocene and Quaternary, may reflect either a higher level of volcanic activity or a shift in prevailing wind directions.

The rest of the section, from 58 to 124 meters, is light brown ferruginous nanno ooze, late Eocene to Oligocene in age. These are the first Eocene sediments found on the Nazca plate, and, together with those at Site 320, the first Oligocene sediments as well. Because some faunas in the upper part of the nanno ooze show dissolution effects, the lithologic transition (to zeolitic clay) probably marks subsidence of the site through the CCD.

Sedimentation rate during deposition of the nanno ooze was 4.0-5.0 m/m.y., compared to 5.0-9.0 m/m.y. for the early Miocene-late Oligocene nanno ooze at Site 320 and 30-40 m/m.y. for that at Site 319. Thus, the sites east of the Galapagos Rise had a lower rate of nanno ooze sedimentation than the one on the west side. Judging from out-of-sequence fossils at Site 319, this difference probably reflects local "ponding" and slumping at Site 319, but there may be real productivity differences as well.

As at Sites 319 and 320, the nanno oozes contain metalliferous components; certain zones contain up to 35% (visual estimates) of RSOs. The RSO percentage may be controlled by the sedimentation rate of calcareous fossils, but is not clearly related to proximity to the Galapagos Rise crest since the highest concentrations are not found at the bases of the sections.

The fossil-based age of the base of the section is 39-40 m.y., the same as the age based on magnetic anomalies (39 m.y.). The radiometric ages on the basalts show considerable variation, with best estimate of about 42 m.y. in essential agreement with the magnetic age. This indicates that sediments began to accumulate at the site almost immediately after the basaltic crust accumulated at the rise crest. The basal sediments contain some basaltic detritus, but most of the section is relatively free of it.

The close correspondence of the paleontological age of the basal sediment, the radiometric age of the basalt, the magnetic anomaly age of the crust, and the Sclater age-depth curve prediction for 4820 meters water depth (38 m.y.) add confidence in using magnetic anomalies and sea-floor depths to predict crustal age in this area of the Nazca plate. Using a half-spreading rate of 7.9 cm/yr, based on the distance between anomalies 12 and 16 near Site 321, and assuming that the Galapagos Rise is 9.5 m.y. old (anomaly 5, according to Herron, 1972), the position of the rise crest, south of the Mendaña Fracture Zone, should be 2400 km southwest of Site 321. Using 8.5 ±1 cm/yr, the minimum permissible rate based on the age of oldest sediment at Site 320 and the known position of the rise crest north of the Mendaña Fracture Zone, the crest south of the fracture zone should be 2900 km from the site. Using either spreading rate, the Galapagos Rise crest cannot be at the location shown by Herron (1972), but must be farther west, as Mammerickx et al. (1975) have suggested from bathymetry.

Basalt

Although both basalt and sediment were recovered in Core 13, the actual contact is not believed to have been recovered. Nonetheless, the abundance of basaltic minerals and altered palagonite in the basal sediments suggests that the contact is depositional. The basalt is relatively uniform from top to bottom of the recovered section, varying from fine-grained, massive, dark gray, almost aphyric basalt at the top to very coarse grained but otherwise identical basalt at the bottom. Subtle variations in grain size suggest at least two cooling units, and this suggestion is augmented by additional data, as discussed below.

On-shore chemical analyses show that the Site 321 basalts, while of the typical spreading ridge type (MORB) in a general sense, are nonetheless significantly enriched in Fe and Ti (the "FeTi basalts" of recent authors; see S.R. Hart, Basement Rock Synthesis, this volume) as well as LIL (large-ion-lithophile) elements. In fact, of the five chemical subgroups established by the shore-lab investigators among the Leg 34 basalts, the thick, lower cooling unit at Site 321 is distinctly the most fractionated or evolved, and the pattern of fractionation is that expected under low pressures. Mineralogically, the high degree of fractionation is expressed in the presence of minor pigeonite, and chemically in the low Al contents of the augites and relatively high Na contents of the plagioclases. The absence of chemical, mineralogical, and textural evidence within this unit for differentiation in situ implies derivation from a highly fractionated magma body in the crust or upper mantle. The unusually abundant amygdules may imply a relatively high volatile content, perhaps another reflection of the highly fractionated nature of the magma; alternatively, or, in addition, the amygdules may reflect eruption at low pressure, which may shed light on the depth of the crest of the Galapagos Rise in late Eocene-early Oligocene times.

Textures are intergranular to almost subophitic in the coarse-grained rocks except for quenched mesostases which suggest rapid cooling, hence flows or shallow sills rather than deep sills. Microphenocrysts are uncommon and almost exclusively plagioclase whose composition, along with those of the rare olivine microphenocrysts, are consistent with fractionated ridge-type tholeiitic magmas. Groundmass olivine (smectite pseudomorphs) indicates that olivine remained on the liquidus to the end, and, hence, that fractionation was not extreme during posteruptive cooling, again consistent with rapidly cooled flows or shallow sills rather than slowly cooled, deeper sills.

Early nonoxidative alteration and later oxidative alteration account for veins and amygdules of smectite, calcite, pyrite, marcasite, and phillipsite, as well as for halmyrolitic titanomaghemite which replaced titanomagnetite in the uppermost part of the thick cooling unit and throughout the thin one.

Water contents of the basalt average 1.21% and range from 0.63 to 1.64%, which are low for DSDP basalt cores. The highest water content was measured in a sample from the thin, upper cooling unit. On the other hand, CO_2 content is high, apparently reflecting the calcite in amygdules. The densities of the basalts increase from 2.75 g/cc at the top to 2.92 g/cc immediately below the top and throughout the rest of the core. The densities and water contents indicate preferential alteration of the thin, upper unit and of the chilled upper contact of the lower unit, and suggest either that the physical integrity of the lower unit prevented deep penetration by diffusion-controlled submarine weathering, or that the finer grained, chilled rocks were somehow more susceptible to alteration, due possibly to a greater content of readily alterable phases (see S.R. Hart, Basement Rock Synthesis, this volume, and M. Bass, Secondary Minerals in Oceanic Basalt, this volume, for more extended discussions).

Remanence inclinations for the basalt suggest the presence of three volcanic flow units, two with reversed and one with normal magnetization. The lower two "magnetic" units, both of reversed polarity, constitute the single, thick, lower unit as inferred from grain size and other petrographic features, and ask the question whether the middle "magnetic" unit is a contact phenomenon of the thick cooling unit, perhaps induced by secondary alteration or, as suggested below, a real record of field inclinations which varied during the finite cooling time of a thick magma unit. In contrast with expectations (and as at Site 319), the coarse-grained flow or sill interior shows the strongest remanent intensity, with the highest single value (333×10^{-4} emu/cm^3) found at any site on Leg 34.

The on-shore investigators distinguish only one chemical subgroup in the basalts from Site 321, in contrast to two subgroups each in those from Sites 319 and 320. The chemical coherence of the Site 321 basalts stems from the fact that all analyses but one were performed on samples from the thick, lower cooling unit to which all but the upper meter of recovered basalt core appear to belong. Strikingly, the single analysis of a sample from the thin upper unit (321-13-4, 119-124 cm; Rhodes et al., Petrology and Chemistry of Basalts from the Nazca plate: Part IV, this volume) is olivine normative, whereas 11 analyses of the lower unit are quartz normative (calculated with the oxidation state of Fe normalized to $Fe^{+3}/(Fe^{+3} + Fe^{+2}) = 0.1$, atomic); indeed, this chemical contrast, which cannot be ascribed to olivine accumulation at the base of the upper unit, controlled the precise placement of the boundary between the proposed cooling units. Further, the only positive magnetic inclination reported for a Site 321 basalt (+22°; Ade-Hall and Johnson Paleomagnetism of Basalts, Leg 34, this volume) was measured on a sample from the thin upper unit. All other inclinations, measured on samples from the lower unit, are negative. Of those, the value on the uppermost sample (321-13-4, 142-145 cm) is so distinct that Ade-Hall and Johnson entertain the possibility that it represents a distinct "middle" time unit. We would stress only that such a time unit need not be an independent eruptive unit, but possibly the chilled margin of the thick flow or shallow sill, as stated above. The remainder of the measured samples from that unit, constituting the third tentative time unit, may have crystallized later, following an abrupt or gradual change of magnetic field inclination; in fact, the great variability of the many measured inclinations in that third time unit may be interpreted as due to continuous or numerous discontinuous changes of inclination. In any case, we again see, as for Sites 319 and 320, permissive to persuasive evidence of at least two time and chemical units in a thin basalt sequence, which again emphasizes the complexity of spreading ridge basalts and the necessity of extensive sampling and analysis if the story in any vertical basalt sequence, even a nominally "thin" one, is to be accurately unraveled.

REFERENCES

Herron, E.M., 1972. Sea floor spreading and Cenozoic history of the East Central Pacific: Geol. Soc. Am. Bull., v. 83, p. 1671-1692.

Kelleher, J.A., 1972. Rupture zones of large South American earthquakes and some predictions: J. Geophys. Res, v. 77, p. 2087-2103.

Mammerickx, J., Anderson, R.N., Menard, H.W., and Smith, S.M., 1975. Morphology and tectonic evolution of the east central Pacific: Geol. Soc. Am. Bull., v. 86, p. 111-118.

Watts, A.B. and Talwani, M., 1974. Gravity anomalies seaward of deep-sea trenches and their tectonic implications: Geophys. J., v. 36, p. 57-90.

Site 321 Hole Core 1 Cored Interval: 0.0-1.5 m

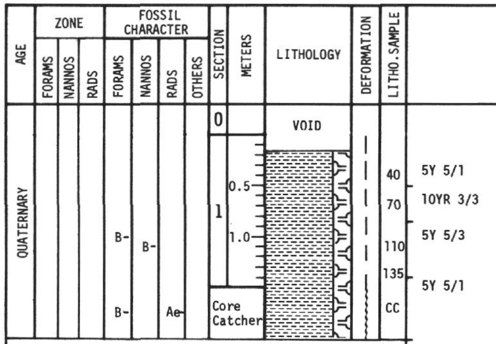

LITHOLOGIC DESCRIPTION

SILICEOUS FOSSIL-RICH DETRITAL CLAY

Core is slightly deformed. Colors are gray (5Y 5/1), olive (5Y 5/3), and dark brown (10YR 3/3). Gray colored clay contains more siliceous fossils.

Characteristic Smear Slides

	1-40	CC
det. clay	70	75
silic. foss.	25	22
nannos	T	T
vol. gls.	2	2
quar + feld	2	1
mica	T	T
heavies	T	T

Grain Size

	1-58
sand	.7
silt	16.9
clay	82.4

Carbon-Carbonate

	1-50
t. carb	0.5
o. carb	0.4
$CaCO_3$	1.0

Bulk X-ray

	1-90
amor	73.0
quar	25.7
K-Fe	2.7
plag	21.9
kaol	6.7
mica	30.1
chlo	4.7
mont	7.6
bari	0.7

Explanatory notes in Chapter 2

Site 321 Hole Core 2 Cored Interval: 1.5-11.0 m

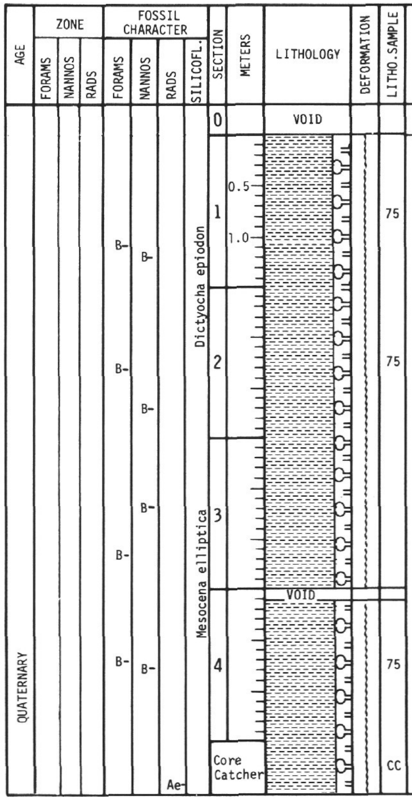

LITHOLOGIC DESCRIPTION

5Y 5/2

SILICEOUS FOSSIL-RICH DETRITAL CLAY

Core is mostly moderately to intensely deformed. Color is olive gray (5Y 5/2).

Characteristic Smear Slides

	1-75	2-75	4-75
det. clay	82	77	70
silic. foss.	15	20	25
nannos	T	-	-
vol. gls.	1	T	-
palag.	T	T	1
quar + feld	1	3	3
pyrite	1	-	T
mica	T	T	1
heavies	T	T	T

Grain Size

	1-50	2-20	3-18	4-28
sand	1.4	0.3	0.3	0.8
silt	18.8	19.2	26.4	30.7
clay	79.8	80.5	73.3	68.5

Carbon-Carbonate

	1-39	2-10	3-9	4-17
t. carb	0.6	0.3	0.4	0.3
o. carb	0.3	0.3	0.3	0.2
$CaCO_3$	2.0	-	-	-

Bulk X-ray

	1-60	2-30	3-34	4-34
amor	74.4	73.3	73.7	76.0
quar	25.7	29.3	28.4	25.8
K-Fe	1.4	1.5	5.5	-
plag	21.3	23.0	21.3	21.7
kaol	4.5	5.1	6.2	2.3
mica	24.7	23.5	21.2	21.9
chlo	4.8	3.7.	2.3	1.4
paly	-	-	-	12.2
mont	16.0	13.9	12.4	11.9
clin	-	-	-	0.5
bari	1.7	-	1.0	0.9
amph	-	-	1.7	1.4

Explanatory notes in Chapter 2

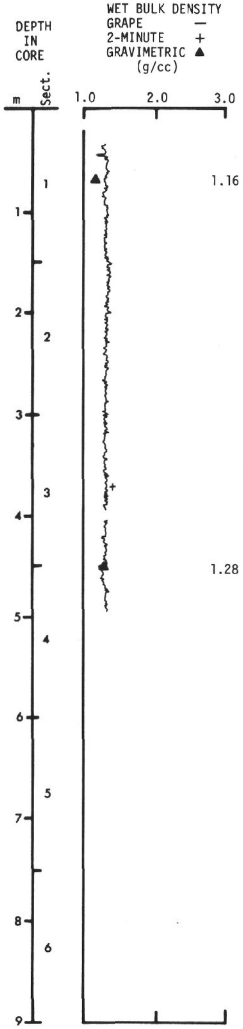

POROSITY (Vol. %)	SONIC VELOCITY, Vp (km/sec)	ACOUSTIC IMPEDANCE ($X10^5$ g/cm^2sec^{-1})	THERMAL CONDUCTIVITY (mcal/cm sec°c)±10%	REMANENT INTENSITY, Jo ($X10^4$ emu/cm^3)	MEAN DEMAGNETIZING FIELD (oe)	INCLINATION BEFORE DEMAGNETIZATION (°)	CLEANED INCLINATION (°)	INITIAL SUSCEPTIBILITY, k ($X10^4$ emu/cm^3 oe)	Q RATIO $\frac{Jo}{0.3k}$	VRM ACQUISITION FACTOR $\frac{\text{moment acquired in time } (t_1-t_2)}{\log (t_1/t_2)}$	SATURATION MAGNETIZATION (emu/g)	CURIE POINT (°c)
87												
	1.52	2.01	1.9									
			1.8									
85												

Site 321 Hole Core 3 Cored Interval: 11.0-20.5 m

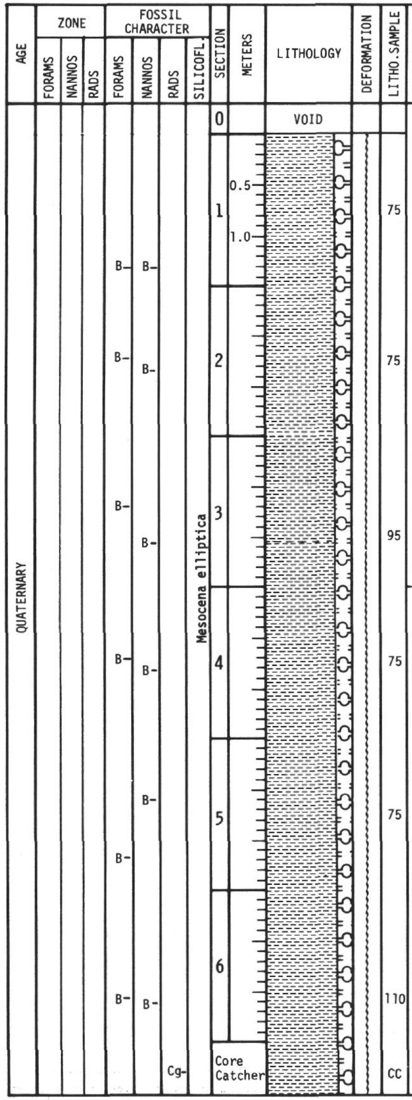

5Y 5/2

N4

5Y 5/2
color change:
olive gray to
grayish green

10GY 5/2
and
5G 5/2

5G 5/2

5Y 5/3

LITHOLOGIC DESCRIPTION

SILICEOUS FOSSIL-RICH DETRITAL CLAY

Core is intensely deformed, and firm to soupy. Colors are olive gray (5Y 5/2) near the top (Sec. 1 and 2) becoming marbled with gray green (10GY 5/2) and (5G 5/2) and finally, in Sec. 6, the color is olive (5Y 5/3).

Characteristic Smear Slides

	1-75	3-95	5-75
det. clay	80	85	85
silic. foss.	15	12	10
vol. gls.	3	1	2
quar + feld	2	2	3
pyrite	-	-	T
mica	T	T	T
heavies	T	T	T

Grain Size

	1-96	2-20	3-20	4-20	5-20	6-28
sand	0.3	0.4	0.3	0.1	0.2	0.3
silt	23.7	28.4	20.8	16.5	19.1	19.2
clay	76.1	71.2	78.9	83.4	80.7	80.5

Carbon-Carbonate

	1-90	2-10	3-14	4-10	5-10	6-18
t. carb	0.4	0.4	0.3	0.7	0.4	0.5
o. carb	0.4	0.4	0.3	0.6	0.4	0.4
$CaCO_3$	1.0	-	-	1.0	-	-

Bulk X-ray

	1-102	4-30
amor	76.6	76.2
quar	27.7	28.0
K-Fe	2.2	0.3
plag	23.9	24.7
kaol	3.8	3.3
mica	25.6	22.1
chlo	1.5	2.1
mont	13.9	15.5
phil	-	3.0
bari	-	1.1
amph	1.5	-

Explanatory notes in Chapter 2

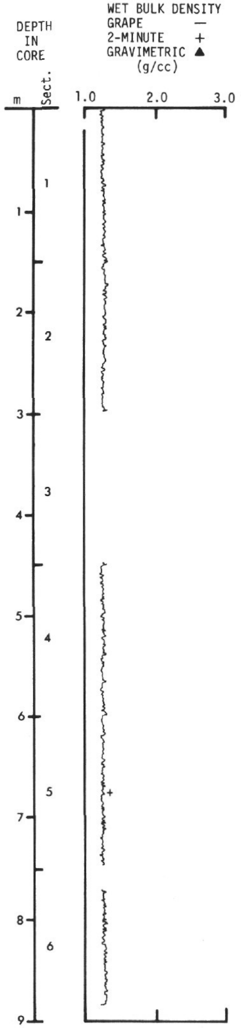

POROSITY (Vol. %)	SONIC VELOCITY, Vp (km/sec)	ACOUSTIC IMPEDANCE ($X10^5$ g/cm^{2}sec^1)	THERMAL CONDUCTIVITY (mcal/cm sec°c)±10%	REMANENT INTENSITY, Jo ($X10^4$ emu/cm^3)	MEAN DEMAGNETIZING FIELD (oe)	INCLINATION BEFORE DEMAGNETIZATION (°)	CLEANED INCLINATION (°)	INITIAL SUSCEPTIBILITY, k ($X10^4$ emu/cm^3 oe)	Q RATIO $\frac{Jo}{0.3k}$	VRM ACQUISITION FACTOR $\frac{\text{moment acquired in time } (t_1-t_2)}{\log (t_1/t_2)}$	SATURATION MAGNETIZATION (emu/g)	CURIE POINT (°c)
	1.52	1.98	1.8 1.8									

Site 321 Hole Core 4 Cored Interval: 20.5-30.0 m

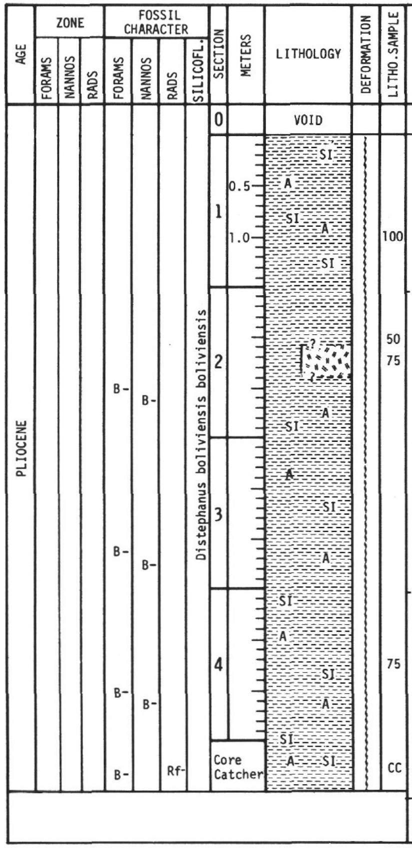

LITHOLOGIC DESCRIPTION

5G 5/2

10GY 5/2

10GY 5/2
and
5Y 5/2

SILICEOUS FOSSIL/VOLCANIC GLASS-BEARING DETRITAL CLAY

Core is intensely deformed throughout. Colors are mostly grayish green (5G 5/2) and (10G 5/2), with some olive gray (5Y 5/2) in Sec. 4. In general, there is a decrease in the amount of siliceous fossils and a small increase in the percentage of clear volcanic glass with depth in the core. Minor lithology in Sec. 2 is a clayey volcanic ash. There are no ash beds; rather, there are zones where volcanic glass is more abundant.

Characteristic Smear Slides

	2-50	2-75	4-75
det. clay	85	43	80
silic. foss.	5	5	10
vol. gls.	7	50	7
quar + feld	3	2	2
opaques	-	-	1

Grain Size

	2-40	3-12	4-18
sand	1.0	0.4	0.3
silt	30.0	25.7	26.0
clay	69.0	73.9	73.7

Carbon-Carbonate

	2-30	3-6	4-9
t. carb	0.4	0.3	0.4
o. carb	0.3	0.3	0.3
$CaCO_3$	-	-	-

Bulk X-ray

	2-50	3-35	4-36
amor	79.1	79.9	76.7
quar	25.1	22.9	21.9
K-Fe	-	1.4	0.9
plag	26.2	24.6	21.0
kaol	5.6	5.8	4.3
mica	21.0	20.3	20.5
chlo	2.6	5.2	2.9
paly	-	-	3.4
mont	18.3	18.2	22.8
clin	0.5	0.5	0.5
bari	-	0.3	0.9
amph	0.7	0.8	0.8

Explanatory notes in Chapter 2

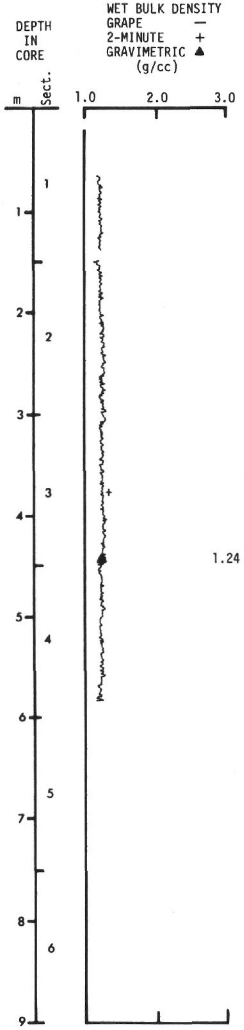

POROSITY (Vol. %)	SONIC VELOCITY, Vp (km/sec)	ACOUSTIC IMPEDANCE ($\times 10^5$ g/cm^{2}sec^1)	THERMAL CONDUCTIVITY (mcal/cm sec°c)±10%	REMANENT INTENSITY, Jo ($\times 10^4$ emu/cm^3)	MEAN DEMAGNETIZING FIELD (oe)	INCLINATION BEFORE DEMAGNETIZATION (°)	CLEANED INCLINATION (°)	INITIAL SUSCEPTIBILITY, k ($\times 10^4$ emu/cm^3 oe)	Q RATIO $\frac{Jo}{0.3k}$	VRM ACQUISITION FACTOR $\frac{\text{moment acquired in time } (t_1 - t_2)}{\log (t_1/t_2)}$	SATURATION MAGNETIZATION (emu/g)	CURIE POINT (°c)
			1.8									
	1.53	1.99	1.8									
90												

Site 321 Hole Core 5 Cored Interval: 30.0-39.5 m

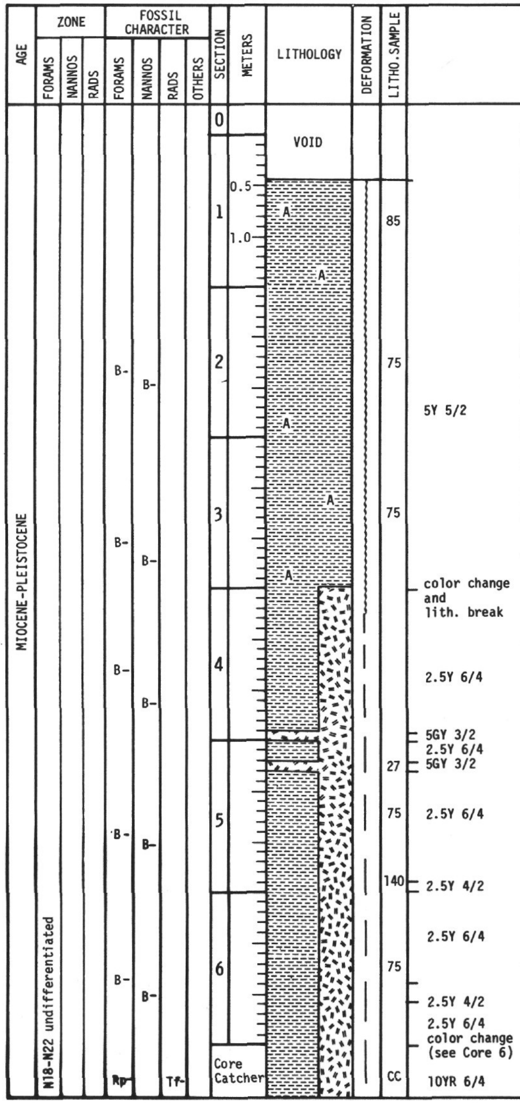

LITHOLOGIC DESCRIPTION

VOLCANIC GLASS-BEARING DETRITAL CLAY AND VOLCANIC GLASS CLAY

Core is roughly divided into two parts by lithology, color, and deformation. The top part (Sec. 1-3) is olive gray (5Y 5/2), intensely deformed, and mostly detrital clay. The bottom part (Sec. 4-6) is light yellowish brown (2.5Y 6/4), dark grayish brown (2.5Y 4/2), and grayish olive green (5GY 3/2) in color, is only slightly deformed, and is a volcanic glass clay and clayey volcanic ash (tuffaceous unit).

Characteristic Smear Slides

	1-85	2-75	5-75
det. clay	85	86	65
silic. foss.	5	2	2
vol. gls.	8	10	30
quar + feld	2	2	3
heavies	T	T	T

Grain Size

	2-30	3-10	4-12	5-18	6-33
sand	1.9	0.3	0.1	0.4	3.6
silt	36.2	26.5	36.1	43.2	65.5
clay	61.8	73.2	63.8	56.4	30.8

Carbon-Carbonate

	2-20	3-10	4-4	5-9	6-10
t. carb	0.3	0.2	0.3	0.2	0.2
o. carb	0.3	0.2	0.3	0.2	0.2
$CaCO_3$	-	-	-	-	-

Bulk X-ray

	2-40	3-19	4-22	5-35	6-19
amor	81.1	79.3	81.4	79.8	88.5
quar	20.4	22.4	21.2	15.3	18.2
K-Fe	1.6	-	-	-	-
plag	24.7	25.7	26.2	37.8	28.9
kaol	3.9	5.4	7.5	2.9	5.9
mica	17.8	18.0	16.6	18.7	16.7
chlo	0.3	3.7	2.0	1.6	5.9
paly	1.8	-	7.0	2.9	5.5
mont	22.1	23.0	18.4	16.0	18.7
clin	0.4	-	-	-	-
phil	4.1	-	-	2.7	-
bari	1.9	0.7	1.1	2.1	-
amph	1.0	1.0	-	-	-

Explanatory notes in Chapter 2

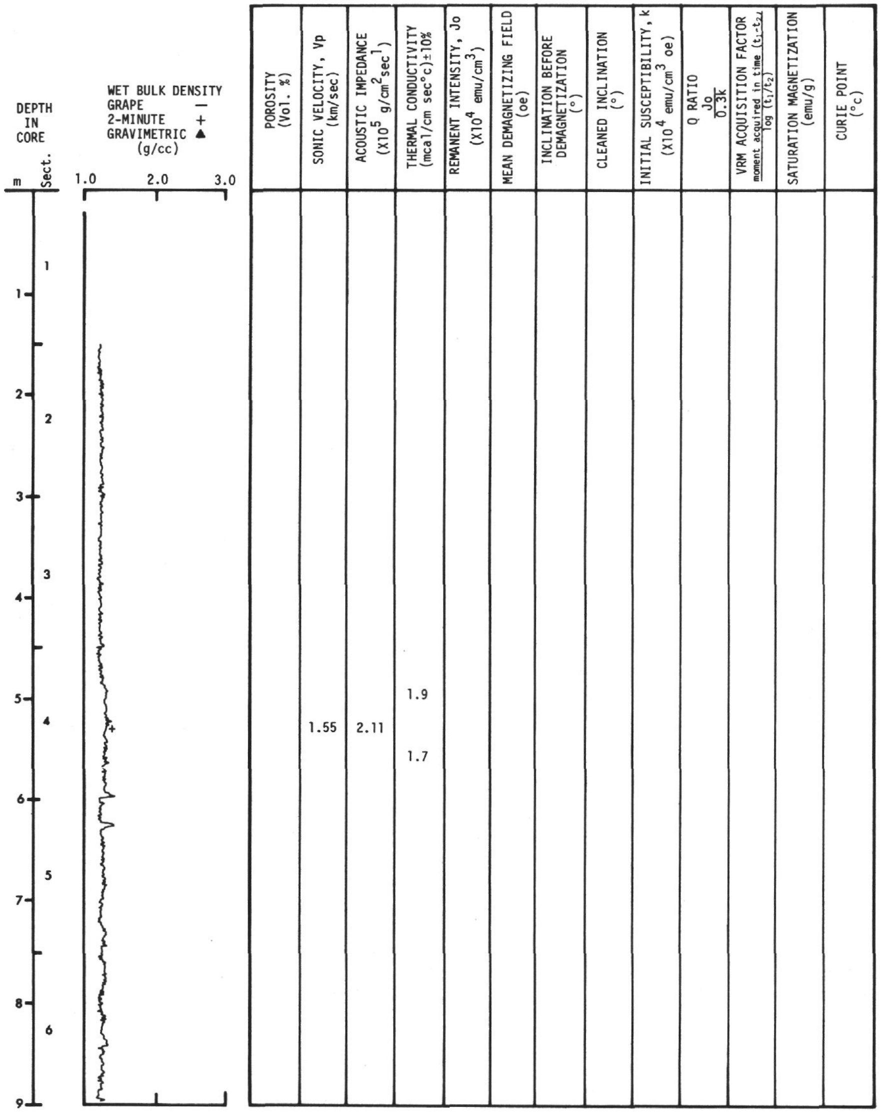

Site 321 Hole Core 6 Cored Interval: 39.5-49.0 m

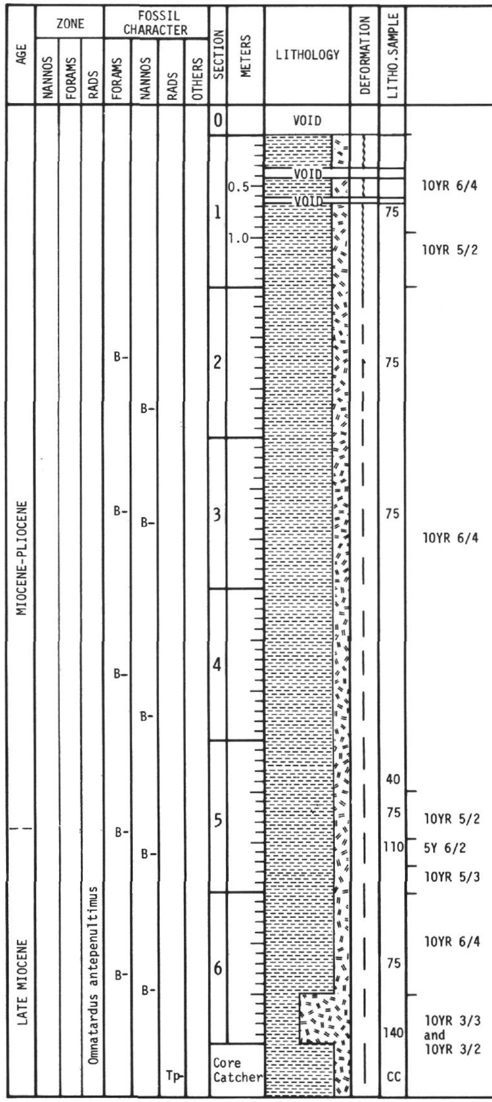

LITHOLOGIC DESCRIPTION

VOLCANIC GLASS-RICH CLAY

Sec. 1 is intensely deformed, whereas the remainder is stiff and only slightly deformed. Colors are light yellowish brown (10YR 6/4) and grayish brown (10YR 5/2) in the top 4 sections and then become more varied with light olive gray (5Y 6/2), brown (10YR 5/3), and dark brown (10YR 3/3) in addition. Of importance in this core is the abundance of fresh clear siliceous volcanic glass within a clayey matrix. The clayey matrix may also be volcanic in origin. There seems to be no close correlation between color and glass content. Minor lithology is clayey volcanic ash.

Characteristic Smear Slides

	1-75	3-75	6-140
det. clay	85	60	37
silic. foss.	T	T	T
nannos	-	10	-
vol. gls.	12	25	55
quar + feld	3	3	3
mica	T	T	T
heavies	T	T	T
opaques	-	2	5

Grain Size

	2-128	3-12	4-14	5-113	6-16
sand	1.5	1.9	1.7	0.2	0.2
silt	49.6	56.0	54.9	36.0	36.6
clay	49.0	42.1	43.4	63.8	63.2

Carbon-Carbonate

	2-142	3-4	4-7	5-6	6-9
t. carb	0.3	0.4	0.2	0.3	0.2
o. carb	0.2	0.2	0.2	0.2	0.2
$CaCO_3$	1.0	2.0	-	1.0	-

Bulk X-ray

	2-113	3-23	4-29	5-28	6-29
amor	81.3	86.0	83.5	78.7	80.7
quar	13.5	15.1	11.5	13.9	10.7
K-Fe	-	-	21.7	17.1	17.3
plag	27.8	28.0	20.4	14.4	18.4
kaol	4.3	4.0	2.8	3.3	5.2
mica	19.1	20.9	31.8	15.2	16.9
chlo	2.8	1.8	-	3.8	1.4
mont	29.8	23.8	11.1	29.8	21.6
phil	1.5	3.6	-	-	4.0
bari	1.2	1.3	0.8	2.5	3.8
amph	-	1.6	-	-	0.8

Core catcher sample contains 2% phillipsite in the very dark grayish brown portion with 10% vol. gls.

Explanatory notes in Chapter 2

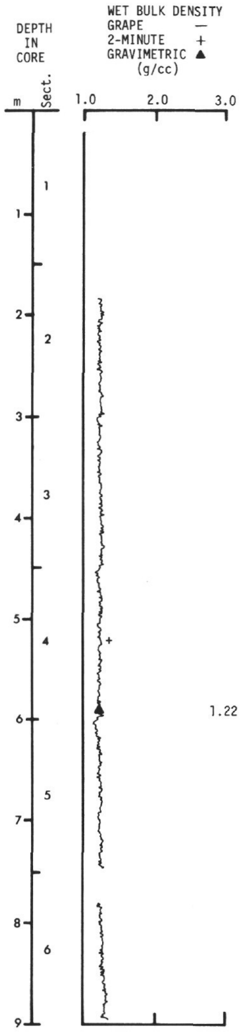

POROSITY (Vol. %)	SONIC VELOCITY, Vp (km/sec)	ACOUSTIC IMPEDANCE ($X10^5$ g/cm^2sec^1)	THERMAL CONDUCTIVITY (mcal/cm sec°c)±10%	REMANENT INTENSITY, Jo ($X10^4$ emu/cm^3)	MEAN DEMAGNETIZING FIELD (oe)	INCLINATION BEFORE DEMAGNETIZATION (°)	CLEANED INCLINATION (°)	INITIAL SUSCEPTIBILITY, k ($X10^4$ emu/cm^3 oe)	Q RATIO $\frac{Jo}{0.3k}$	VRM ACQUISITION FACTOR $\frac{\text{moment acquired in time } (t_1-t_2)}{\log (t_1/t_2)}$	SATURATION MAGNETIZATION (emu/g)	CURIE POINT (°c)
			1.9									
	1.54	2.00										
91												

Site 321 Hole Core 7 Cored Interval: 49.0-58.5 m

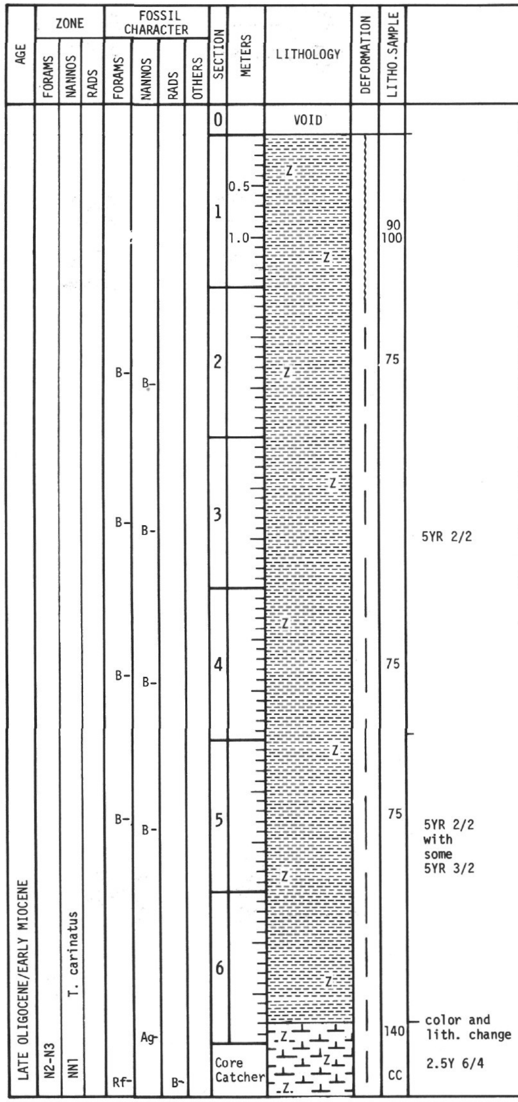

Explanatory notes in Chapter 2

LITHOLOGIC DESCRIPTION

ZEOLITE-BEARING BROWN CLAY

Top section is intensely deformed, whereas the remaining sections are stiff and only slightly deformed. Color is mainly dark brown (5YR 2/2), with some intermixed grayish brown (5YR 3/2) in Sec. 5 and 6 and a color change to light yellowish brown (2.5Y 6/4) near the base of Sec. 6. ZEOLITE-BEARING NANNO OOZE becomes major lithology near base of Sec. 6.

Characteristic Smear Slides

	1-90	2-75	4-75	CC
clay	90	88	87	5
RSO + opaq.	3	5	3	3
nannos	-	-	T	82
phil	3	6	7	10
quar + feld	4	1	2	T
mica	T	T	1	-
heavies	T	T	-	-

Grain Size

	2-41	3-13	4-17	5-7	6-12
sand	0.1	0.1	0.0	0.1	0.0
silt	23.2	23.7	32.8	32.1	29.8
clay	76.7	76.2	67.2	67.9	70.2

Carbon-Carbonate

	2-35	3-7	4-8	5-2	6-6	6-147
t. carb	0.1	0.1	0.2	0.2	0.2	10.7
o. carb	0.1	0.1	0.1	0.1	0.1	-
$CaCO_3$	-	-	-	-	-	89.0

Bulk X-ray

	2-44	3-27	4-33	5-20	6-17
amor	77.6	74.8	72.9	70.6	70.5
feld	32.3	23.3	19.6	12.3	7.2
quar	14.7	13.6	18.2	10.0	9.2
kaol	2.7	3.3	1.1	-	-
mica	18.0	20.4	23.3	17.2	15.4
chlo	-	2.6	1.6	-	2.5
goet	-	-	3.9	22.4	25.1
mont	17.6	15.9	4.4	8.6	9.1
clin	1.8	0.6	0.9	-	0.7
phil	12.9	19.4	27.0	29.5	30.2
amph	-	1.0	-	-	0.7

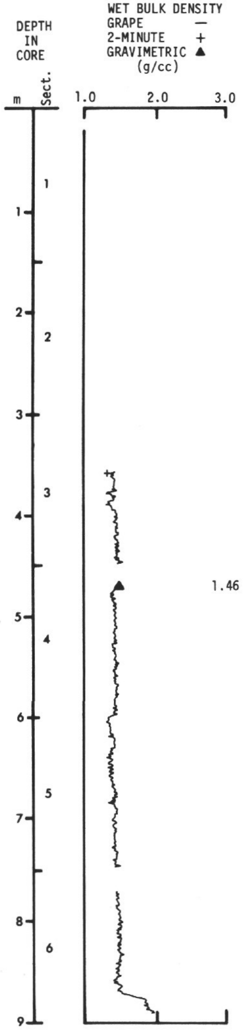

POROSITY (Vol. %)	SONIC VELOCITY, Vp (km/sec)	ACOUSTIC IMPEDANCE $(X10^5\ g/cm^2sec^1)$	THERMAL CONDUCTIVITY (mcal/cm sec°c)±10%	REMANENT INTENSITY, Jo $(X10^4\ emu/cm^3)$	MEAN DEMAGNETIZING FIELD (oe)	INCLINATION BEFORE DEMAGNETIZATION (°)	CLEANED INCLINATION (°)	INITIAL SUSCEPTIBILITY, k $(X10^4\ emu/cm^3\ oe)$	Q RATIO $\frac{Jo}{0.3k}$	VRM ACQUISITION FACTOR $\frac{\text{moment acquired in time } (t_1-t_2)}{\log (t_1/t_2)}$	SATURATION MAGNETIZATION (emu/g)	CURIE POINT (°c)
			1.9									
	1.54	2.03										
			1.9									
81												
				0.12		+09	+19					

Site 321 Hole Core 8 Cored Interval: 58.5-68.0 m

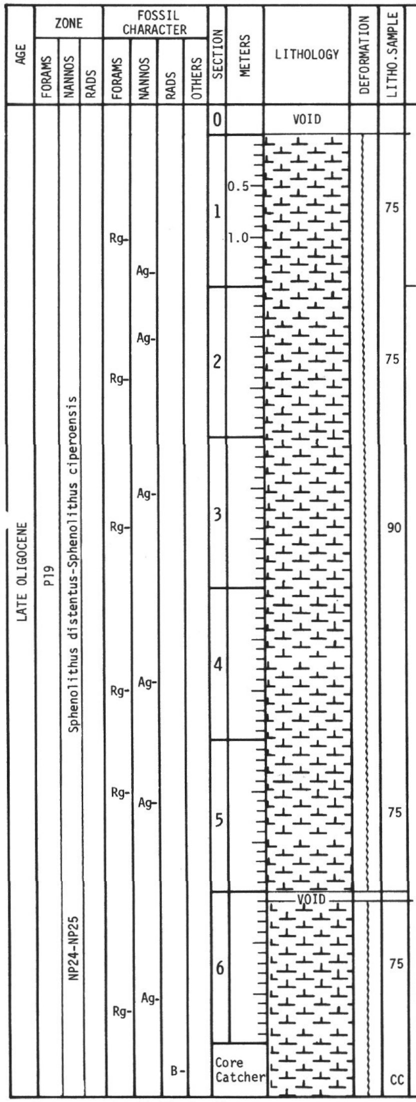

LITHOLOGIC DESCRIPTION

2.5Y 7/4

2.5Y 7/3

2.5Y 5/4

NANNO OOZE

Core is intensely deformed and is watery in places. Colors are pale yellow (2.5Y 7/4 and 2.5Y 7/3) and lighter pale yellow near base (2.5Y 5/4).

Characteristic Smear Slides

	1-75	6-75
clay	T	T
RSO	1	1
nannos	90	90
micarb	4	4
forams	5	5
phil	-	T

Grain Size

	1-19	2-20	3-34	4-17	5-123	6-21
sand	0.0	0.0	0.0	0.0	0.0	0.0
silt	59.6	57.5	58.1	55.5	57.2	57.8
clay	40.4	42.5	41.8	44.5	42.8	42.2

Carbon-Carbonate

	1-30	2-14	3-12	4-33	5-135	6-15
t. carb	11.4	11.4	11.4	11.4	11.2	11.4
o. carb	-	0.1	-	-	-	-
$CaCO_3$	95.0	95.0	94.0	95.0	93.0	95.0

Bulk X-ray

	1-46	4-43
amor	17.3	16.1
calc	100.0	100.0

Explanatory notes in Chapter 2

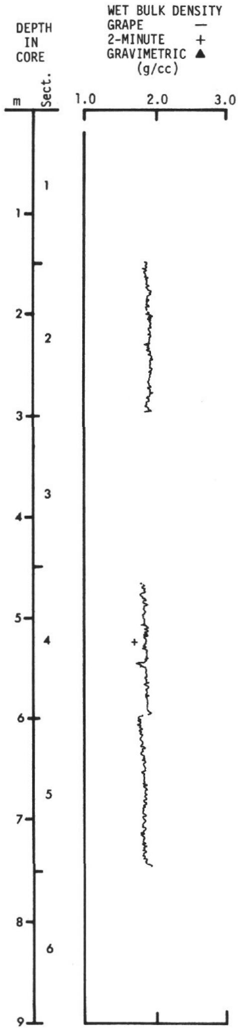

POROSITY (Vol. %)	SONIC VELOCITY, Vp (km/sec)	ACOUSTIC IMPEDANCE ($X10^5$ g/cm^2sec^1)	THERMAL CONDUCTIVITY (mcal/cm sec°c)±10%	REMANENT INTENSITY, Jo ($X10^4$ emu/cm^3)	MEAN DEMAGNETIZING FIELD (oe)	INCLINATION BEFORE DEMAGNETIZATION (°)	CLEANED INCLINATION (°)	INITIAL SUSCEPTIBILITY, k ($X10^4$ emu/cm^3 oe)	Q RATIO $\frac{Jo}{0.3k}$	VRM ACQUISITION FACTOR $\frac{\text{moment acquired in time } (t_1-t_2)}{\log (t_1/t_2)}$	SATURATION MAGNETIZATION (emu/g)	CURIE POINT (°c)
	1.56	2.75	2.3									

Site 321 Hole Core 9 Cored Interval: 68.0-77.5 m

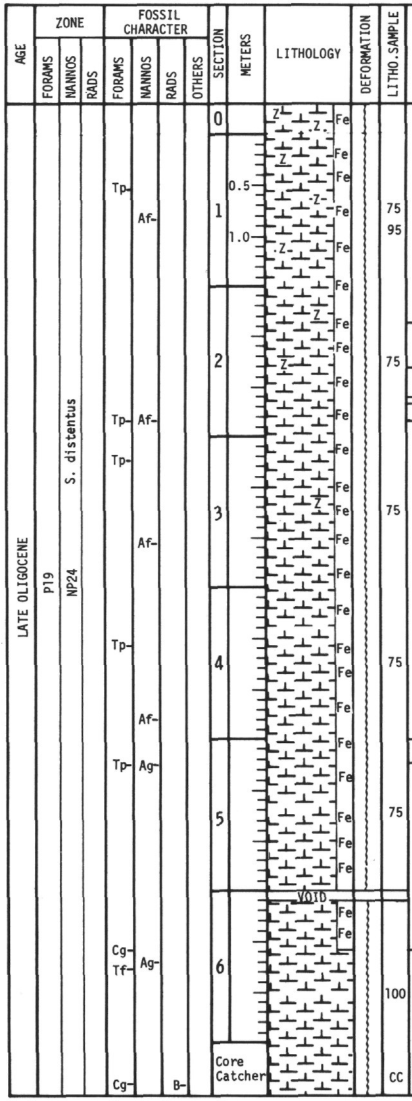

Explanatory notes in Chapter 2

LITHOLOGIC DESCRIPTION

10YR 3/3 and 10YR 6/4

10YR 6/4

10YR 5/4

10YR 4/4

10YR 6/4

10YR 5/4 and some 10YR 4/4

10YR 4/4

10YR 3/3

10YR 6/6

IRON/ZEOLITE-RICH NANNO OOZE

Core is intensely deformed. Colors are various browns and yellow browns, including dark brown (10YR 3/3), dark to light yellow brown (10YR 4/4, 10YR 5/4, and 10YR 6/4), and brownish yellow (10YR 6/6). Core is mostly a nanno ooze which has decreasing amounts of zeolite with depth and a high RSO content in the darker colors. Bottom of core is NANNO OOZE.

Characteristic Smear Slides

	1-75	5-75	6-100
clay	T	T	T
RSO	10	20	2
nannos	70	65	85
micarb	5	5	5
forams	T	2	5
phil	15	3	3

Grain Size

	1-69	2-94	3-52	4-85	5-7	6-43
sand	0.1	0.1	0.1	0.0	0.0	0.1
silt	39.5	46.2	39.6	33.0	42.3	27.9
clay	60.3	53.8	60.3	67.0	57.6	72.0

Carbon-Carbonate

	1-98	2-112	3-65	4-66	5-4	6-49
t. carb	6.8	9.2	9.9	9.0	9.5	6.4
o. carb	0.1	0.1	0.1	0.1	0.1	0.1
$CaCO_3$	56.0	76.0	82.0	74.0	78.0	52.0

Bulk X-ray

	1-118	4-113	5-44	6-58
amor	35.0	42.5	49.2	26.8
calc	83.0	87.5	78.5	95.5
feld	4.3	1.6	1.7	-
quar	1.5	1.1	1.4	0.4
goet	7.1	9.9	17.0	4.1
phil	4.0	-	1.4	-

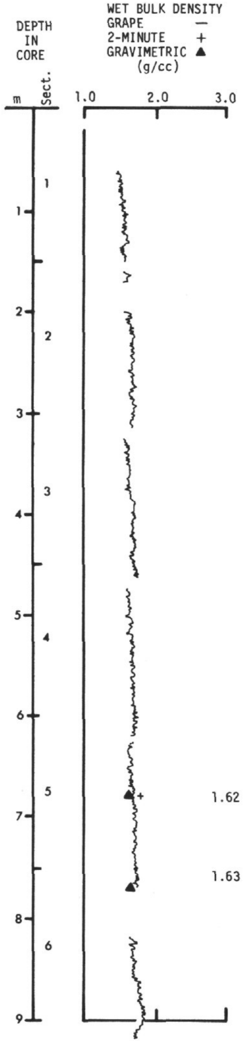

POROSITY (Vol. %)	SONIC VELOCITY, Vp (km/sec)	ACOUSTIC IMPEDANCE ($X10^5$ g/cm^2sec^1)	THERMAL CONDUCTIVITY (mcal/cm sec°c)±10%	REMANENT INTENSITY, Jo ($X10^4$ emu/cm^3)	MEAN DEMAGNETIZING FIELD (oe)	INCLINATION BEFORE DEMAGNETIZATION (°)	CLEANED INCLINATION (°)	INITIAL SUSCEPTIBILITY, k ($X10^4$ emu/cm^3 oe)	Q RATIO $\frac{Jo}{0.3k}$	VRM ACQUISITION FACTOR $\frac{\text{moment acquired in time } (t_1-t_2)}{\log (t_1/t_2)}$	SATURATION MAGNETIZATION (emu/g)	CURIE POINT (°c)
				0.08		+05	+04					
			2.2									
66	1.51	2.52										
			2.2									
67												
				0.21		+06	+14					

Site 321 Hole Core 10 Cored Interval: 77.5-87.0 m

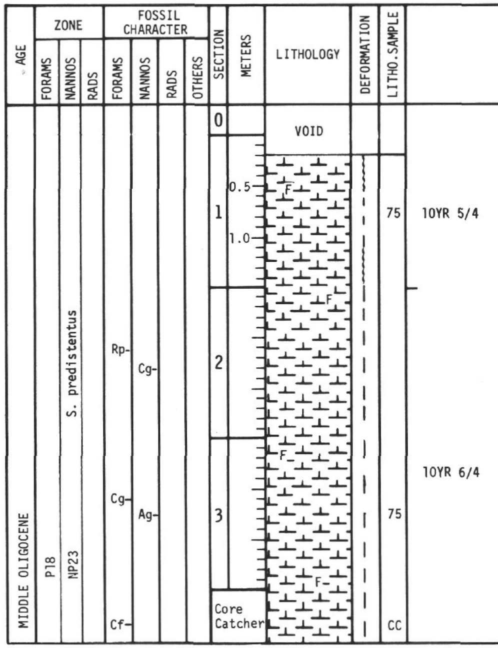

LITHOLOGIC DESCRIPTION

NANNO OOZE

Core is only slightly disturbed throughout Sec. 2 and 3, moderately deformed in Sec. 1. Colors are yellowish brown (10YR 5/4 and 10YR 6/4).

Characteristic Smear Slides

	1-75	3-75
clay	T	T
RSO	5	3
nannos	75	85
micarb	10	10
forams	7	1
phil	3	1

Grain Size

	1-93	2-22	3-20
sand	0.1	0.0	0.1
silt	46.0	48.3	49.6
clay	53.9	51.6	50.3

Carbon-Carbonate

	1-100	2-10	3-10
t. carb	10.8	11.0	11.1
o. carb	0.1	0.1	0.1
$CaCO_3$	90.0	91.0	92.0

Bulk X-ray

	1-84	2-30	3-30
amor	23.5	23.6	23.3
calc	96.0	97.9	96.7
quar	-	0.3	0.2
goet	4.0	1.9	2.4
phil	-	-	0.7

Explanatory notes in Chapter 2

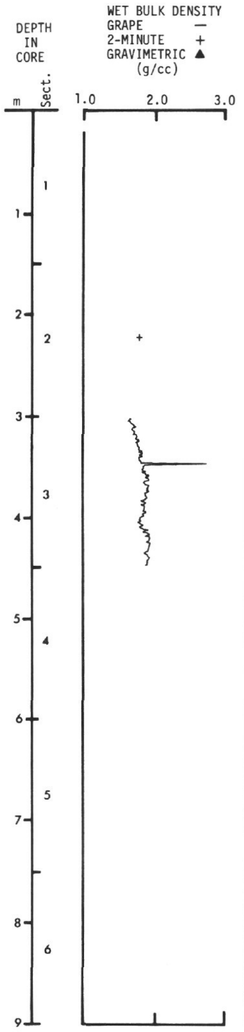

POROSITY (Vol. %)	SONIC VELOCITY, Vp (km/sec)	ACOUSTIC IMPEDANCE ($X10^5$ g/cm^{2}sec^{-1})	THERMAL CONDUCTIVITY (mcal/cm sec°c)±10%	REMANENT INTENSITY, Jo ($X10^4$ emu/cm^3)	MEAN DEMAGNETIZING FIELD (oe)	INCLINATION BEFORE DEMAGNETIZATION (°)	CLEANED INCLINATION (°)	INITIAL SUSCEPTIBILITY, k ($X10^4$ emu/cm^3 oe)	Q RATIO $\frac{Jo}{0.3k}$	VRM ACQUISITION FACTOR moment acquired in time (t_1-t_2) / $\log(t_1/t_2)$	SATURATION MAGNETIZATION (emu/g)	CURIE POINT (°c)
			2.1									
	1.54	2.71										
			2.4	0.04		-02	+05					
				0.03		-04	+03					

Site 321 Hole Core 11 Cored Interval: 87.0-96.5 m

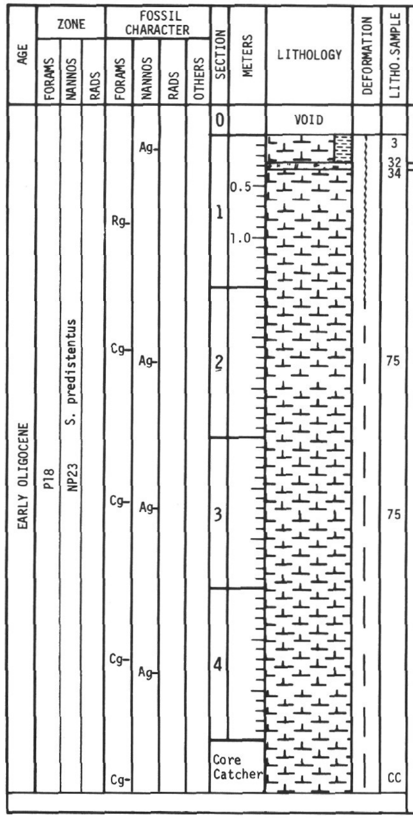

varicolored
10YR 2.5/1

10YR 6/6
and
10YR 7/6

LITHOLOGIC DESCRIPTION

NANNO OOZE

Core is intensely deformed in Sec. 1, only slightly deformed in Sec. 2-4. Sec. 1 is most diverse in lithology and in color, with 0-29 cm interval of very dark brown (10YR 2.5/2) zeolitic brown clay and yellow brown (10YR 6/6) nanno ooze, and a 6 cm bed (29-35 cm) of black (10YR 2.5/1) and grayish-green (10GY 5/2) devitrified ash (bentonite). The bottom part of Sec. 1 and Sec. 2-4 are light yellowish brown (10YR 6/6 and 10YR 7/6) nanno ooze.

Characteristic Smear Slides

	1-34	2-75	4-75
clay	55	1	2
RSO	-	T	2
nannos	2	90	85
micarb	-	6	3
forams	-	3	8
phil	-	-	-
palag.	43	-	-

Grain Size

	1-54	2-20	3-20	4-18
sand	0.1	0.1	0.3	0.1
silt	54.9	52.0	54.1	51.7
clay	45.0	47.9	45.6	48.2

Carbon-Carbonate

	1-48	2-10	3-10	4-7
t. carb	11.2	11.2	11.0	11.0
o. carb	0.1	0.1	0.1	0.1
$CaCO_3$	93.0	93.0	92.0	91.0

Bulk X-ray

	1-30	2-30	3-30	4-26
amor	79.8	20.5	19.7	21.3
calc	-	98.6	98.2	98.2
quar	8.6	-	-	-
K-Fe	2.8	-	-	-
plag	17.7	-	-	-
kaol	1.7	-	-	-
mica	7.6	-	-	-
goet	10.9	1.4	1.8	1.8
mont	47.3	-	-	-
phil	3.3	-	-	-

Site 321 Hole Core 12 Cored Interval: 106.0-115.5 m

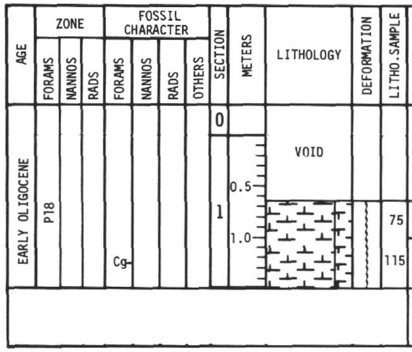

10YR 7/4

10YR 4/4

LITHOLOGIC DESCRIPTION

FORAM-RICH NANNO OOZE

Core liner collapsed during coring; section is extremely disturbed. Colors are very pale brown (10YR 7/4) and dark yellowish brown (10YR 4/4).

Characteristic Smear Slide

	1-85
clay	T
RSO	3
nannos	70
micarb	10
forams	15
phil	2

Explanatory notes in Chapter 2

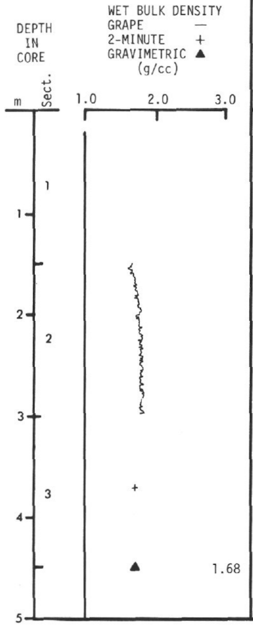

POROSITY (Vol. %)	SONIC VELOCITY, Vp (km/sec)	ACOUSTIC IMPEDANCE ($X10^5$ g/cm^2sec^1)	THERMAL CONDUCTIVITY (mcal/cm sec°c)±10%	REMANENT INTENSITY, Jo ($X10^4$ emu/cm^3)	MEAN DEMAGNETIZING FIELD (oe)	INCLINATION BEFORE DEMAGNETIZATION (°)	CLEANED INCLINATION (°)	INITIAL SUSCEPTIBILITY, k ($X10^4$ emu/cm^3 oe)	Q RATIO $\frac{Jo}{0.3k}$	VRM ACQUISITION FACTOR $\frac{\text{moment acquired in time } (t_1-t_2)}{\log (t_1/t_2)}$	SATURATION MAGNETIZATION (emu/g)	CURIE POINT (°c)
				0.05		+06	+07					
				0.09		+11	+18					
				0.02		+02	+12					
			3.1									
	1.57	2.76										
			2.5									
59												
				0.04		+05	+09					

Site 321 Hole Core 13 Cored Interval: 115.5-125.0 m

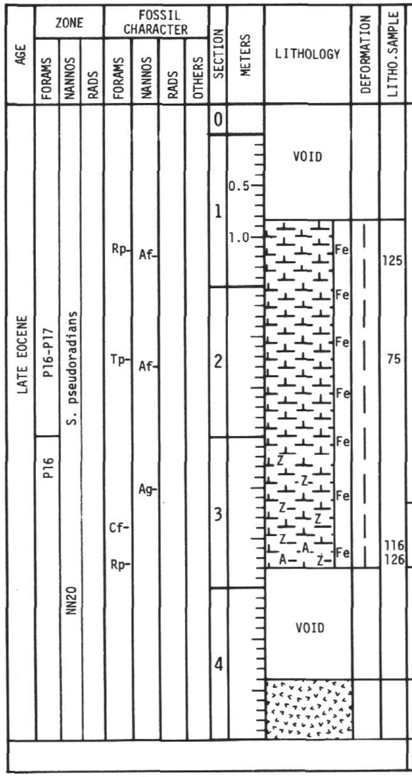

LITHOLOGIC DESCRIPTION

IRON-RICH NANNO OOZE AND BASALT

Sediment core is only slightly deformed. *Color of sediment is dark grayish brown* (10YR 3/2 and 10YR 3/3). Contact of nanno ooze and basalt is at 3-130. Void in the bottom part of Sec. 3 and the top of Sec. 4 is artificial; core catcher material and bottom of Sec. 3 were included in a new Sec. 4. There is an increase in phillipsite and green devitrified glass nontronite(?) contents directly above the contact.

10YR 3/2

Characteristic Smear Slides

	1-125	3-116	3-125	3-126
clay	3	5	T	5
RSO	10	15	15	15
nannos	80	70	70	50
micarb	7	2	7	3
forams	T	-	-	-
phil	T	3	5	12
vol. gls.	-	1	-	-
palag.	-	3	3	15
feld	-	1	T	T

10YR 3/3

Grain Size

	1-90	2-20	3-16
sand	0.1	0.0	0.1
silt	70.9	70.5	69.9
clay	29.0	29.5	30.0

Carbon-Carbonate

	1-88	2-14	3-10
t. carb	10.4	10.1	9.8
o. carb	0.1	0.1	0.1
$CaCO_3$	86.0	84.0	81.0

N4

Bulk X-ray

	1-94	2-35	3-116
amor	32.0	38.3	43.1
calc	95.6	94.4	93.4
quar	0.2	0.2	-
goet	4.2	5.3	4.0
phil	-	-	2.6

Explanatory notes in Chapter 2

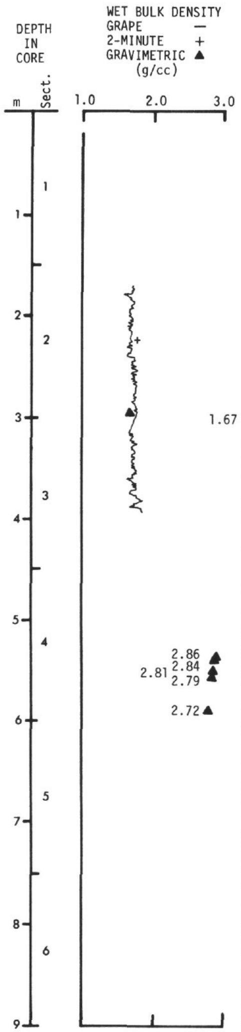

POROSITY (Vol. %)	SONIC VELOCITY, Vp (km/sec)	ACOUSTIC IMPEDANCE ($X10^5$ g/cm^2sec^1)	THERMAL CONDUCTIVITY (mcal/cm sec°c)±10%	REMANENT INTENSITY, Jo ($X10^4$ emu/cm^3)	MEAN DEMAGNETIZING FIELD (oe)	INCLINATION BEFORE DEMAGNETIZATION (°)	CLEANED INCLINATION (°)	INITIAL SUSCEPTIBILITY, k ($X10^4$ emu/cm^3 oe)	Q RATIO $\frac{Jo}{0.3k}$	VRM ACQUISITION FACTOR $\frac{\text{moment acquired in time }(t_1-t_2)}{\log(t_1/t_2)}$	SATURATION MAGNETIZATION (emu/g)	CURIE POINT (°c)
				0.06		-08	+25					
			2.6									
	1.54	2.60										
			2.6	0.02		+04	+37					
65												
				0.02		-12	-21					
	5.28	14.8		13.0	265	+24	+22	9.7	4.5		1.0	287
				3.90		-25	-22	11.3	1.1	10^{62}	0.33	319

Site 321 Hole Core 14 Cored Interval: 125.0-134.5 m

AGE	ZONE			FOSSIL CHARACTER				SECTION	METERS	LITHOLOGY	DEFORMATION	LITHO.SAMPLE	LITHOLOGIC DESCRIPTION
	FORAMS	NANNOS	RADS	FORAMS	NANNOS	RADS	OTHERS						
								0		VOID			
								1	0.5 1.0	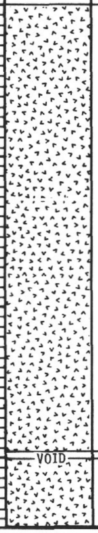			BASALT Original recovery about 5 meters. Core appears longer because of styrofoam spacers that are used to separate parts of the cores. See individual section descriptions for petrography and some interpretations.
								2					N4
								3		VOID			

Explanatory notes in Chapter 2

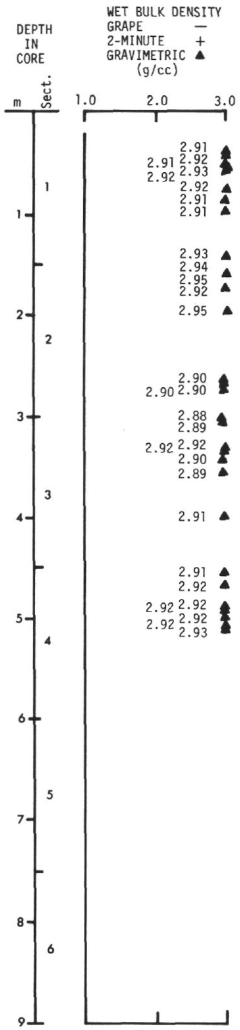

POROSITY (Vol. %)	SONIC VELOCITY, Vp (km/sec)	ACOUSTIC IMPEDANCE ($X10^5$ g/cm^{2}sec^1)	THERMAL CONDUCTIVITY (mcal/cm sec°c)±10%	REMANENT INTENSITY, Jo ($X10^4$ emu/cm^3)	MEAN DEMAGNETIZING FIELD (oe)	INCLINATION BEFORE DEMAGNETIZATION (°)	CLEANED INCLINATION (°)	INITIAL SUSCEPTIBILITY, k ($X10^4$ emu/cm^3 oe)	Q RATIO $\frac{Jo}{0.3k}$	VRM ACQUISITION FACTOR $\frac{\text{moment acquired in time } (t_1-t_2)}{\log (t_1/t_2)}$	SATURATION MAGNETIZATION (emu/g)	CURIE POINT (°c)
	6.06	17.7		45 122 62.6 47.8 83.5 135 120	100 65 75 110 105 110 200(T)	+10 +14 -08 00 -05 -06 -10	-13 -10 -10 -12 -08 -11 -07	45.9 43.1 22.9 17 51.3 19.0	3.3 9.4 8.8 5.4 22.9	10^3 10^{45}	2.2 1.37 1.9 1.7	208 162 135 146 163
				140 137 172	115(T) 135 80	-07 -03 -17	-08 -16 -23	49.0 49.0	9.3 12	10^{70}	1.9 2.0	149 157
				102 163	70	-26 -12	-21 -22	27.5	13 19.1	10^5	1.41	150 150
				91	75	-17	-14	34		10^{32}		
				94 64.6	45 35	+04 -10	-22 -20	95.3 45.8	3.3 4.5		2.0 1.43	120 136
				56.4 55.8	40 60	-12 -02	-39 -16	55 37.9	4.7	10^2	1.55	125 160
				333 61.1 81.0	25 75 60	+01 -09 +01	-13 -12 -19	58.9 44.1 65.1	19 4.6 4.2		3.0 0.16 2.2	176 157 157
				110 90.0	45 55	-16 -07	-10 -16	53 38.2	7.6	10^{24}	1.39	136
	5.72	16.7		77.9 90.0 140 117 100 84.6	90(T) 55 40 70 40	-11 -22 -10 -14 -01 -12	-25 -19 -14 -21 -21 -14	59 121 49.4 91.5 50.7	2.5 7.6 3.6 5.4	10^5 10^{51}	6.7 1.36 1.9 1.44	140 125 125 125 127

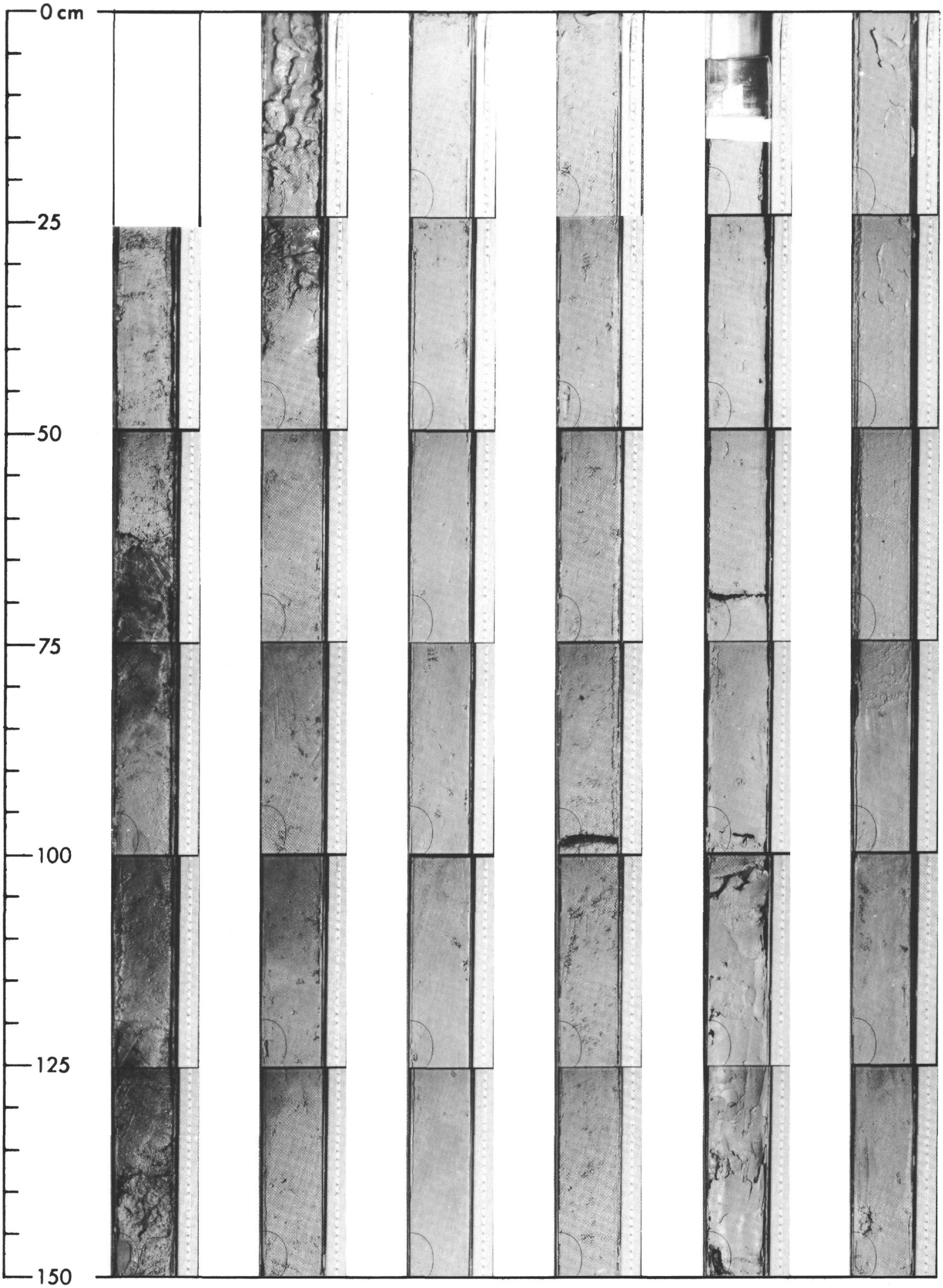

0 cm
25
50
75
100
125
150
321-1-1
321-2-1
321-2-2
321-2-3
321-2-4
321-3-1

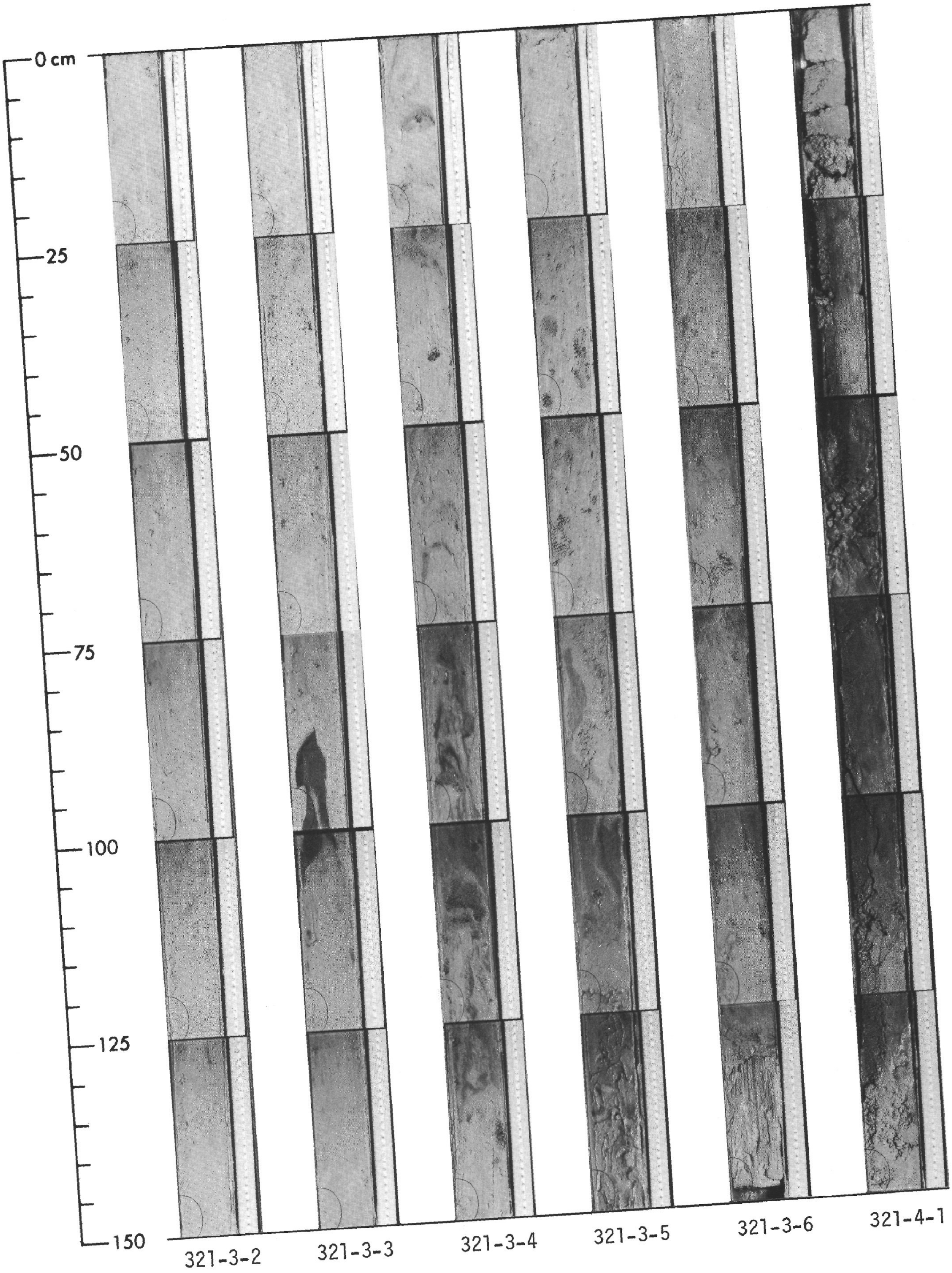
0 cm
25
50
75
100
125
150
321-3-2
321-3-3
321-3-4
321-3-5
321-3-6
321-4-1

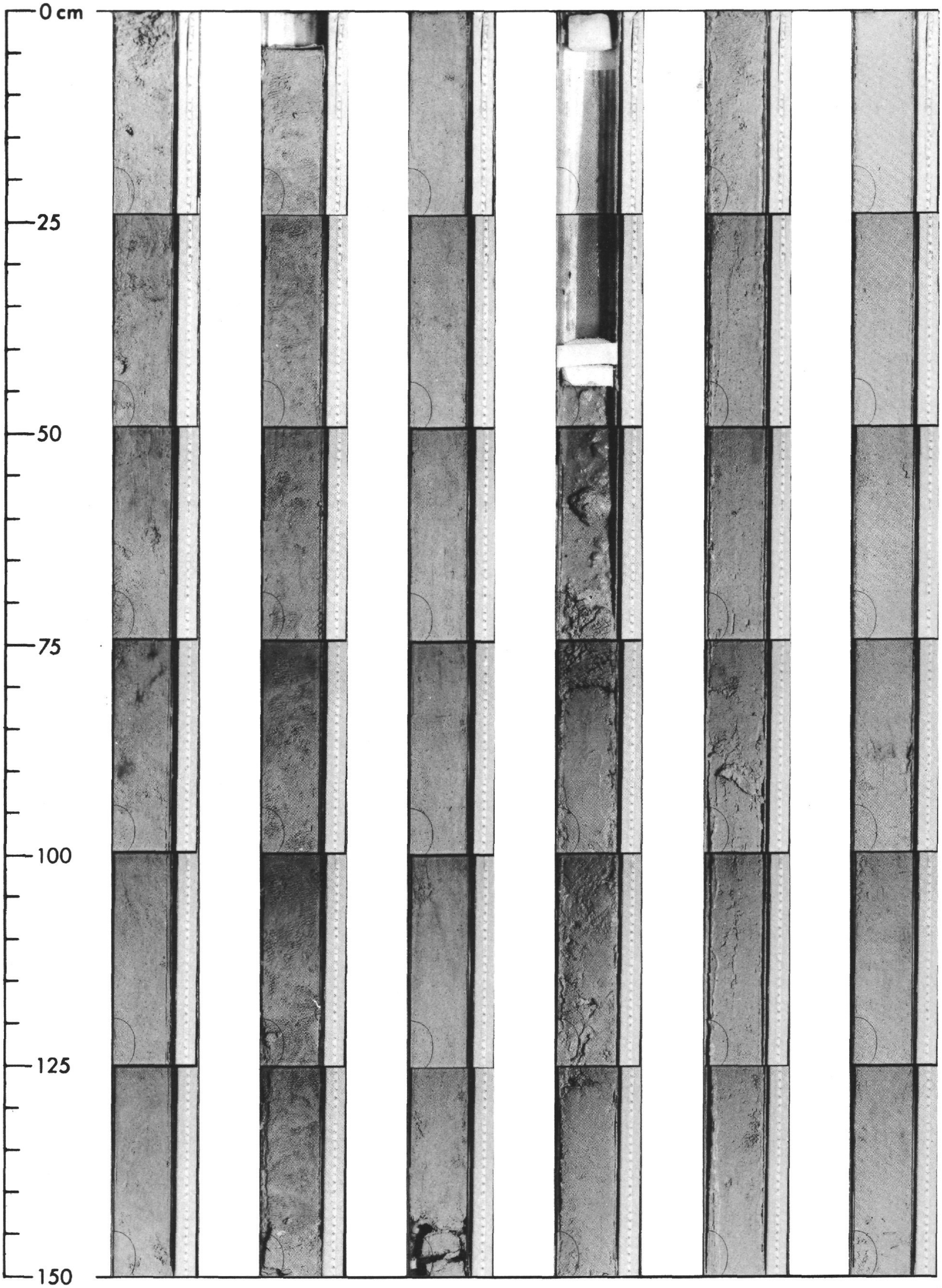
0 cm
25
50
75
100
125
150
321-4-2
321-4-3
321-4-4
321-5-1
321-5-2
321-5-3

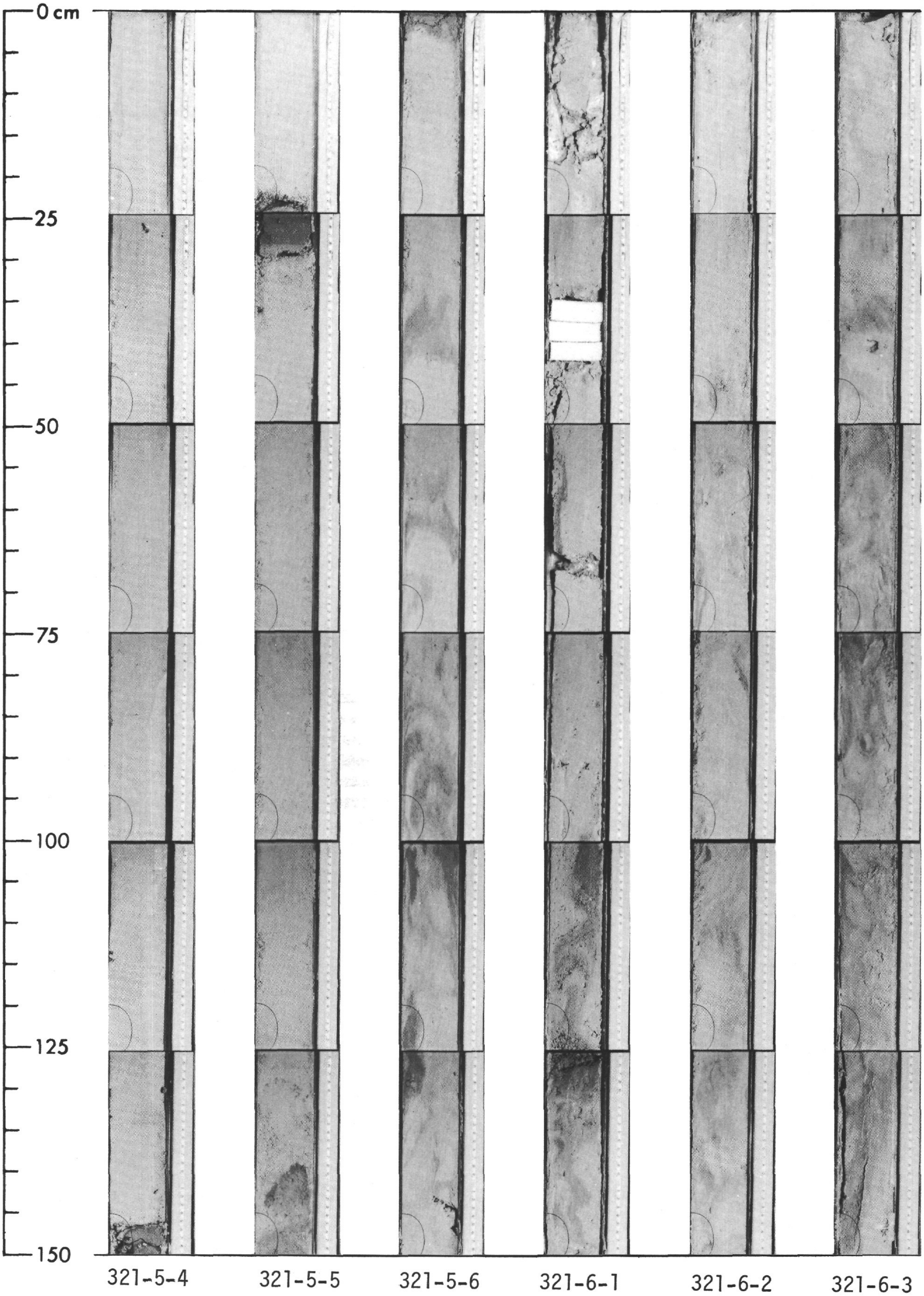
0 cm
25
50
75
100
125
150
321-5-4
321-5-5
321-5-6
321-6-1
321-6-2
321-6-3

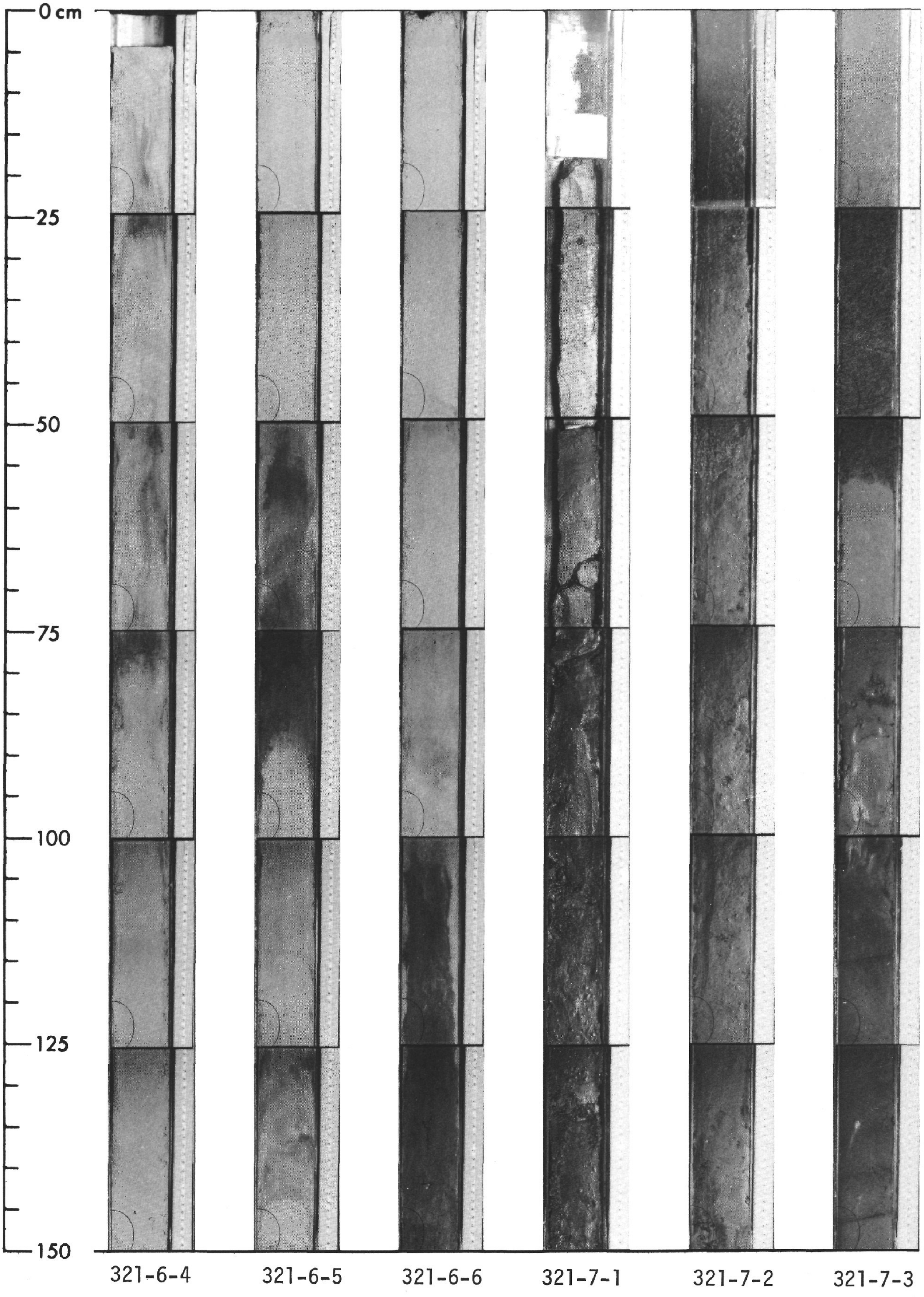
0 cm
25
50
75
100
125
150
321-6-4
321-6-5
321-6-6
321-7-1
321-7-2
321-7-3

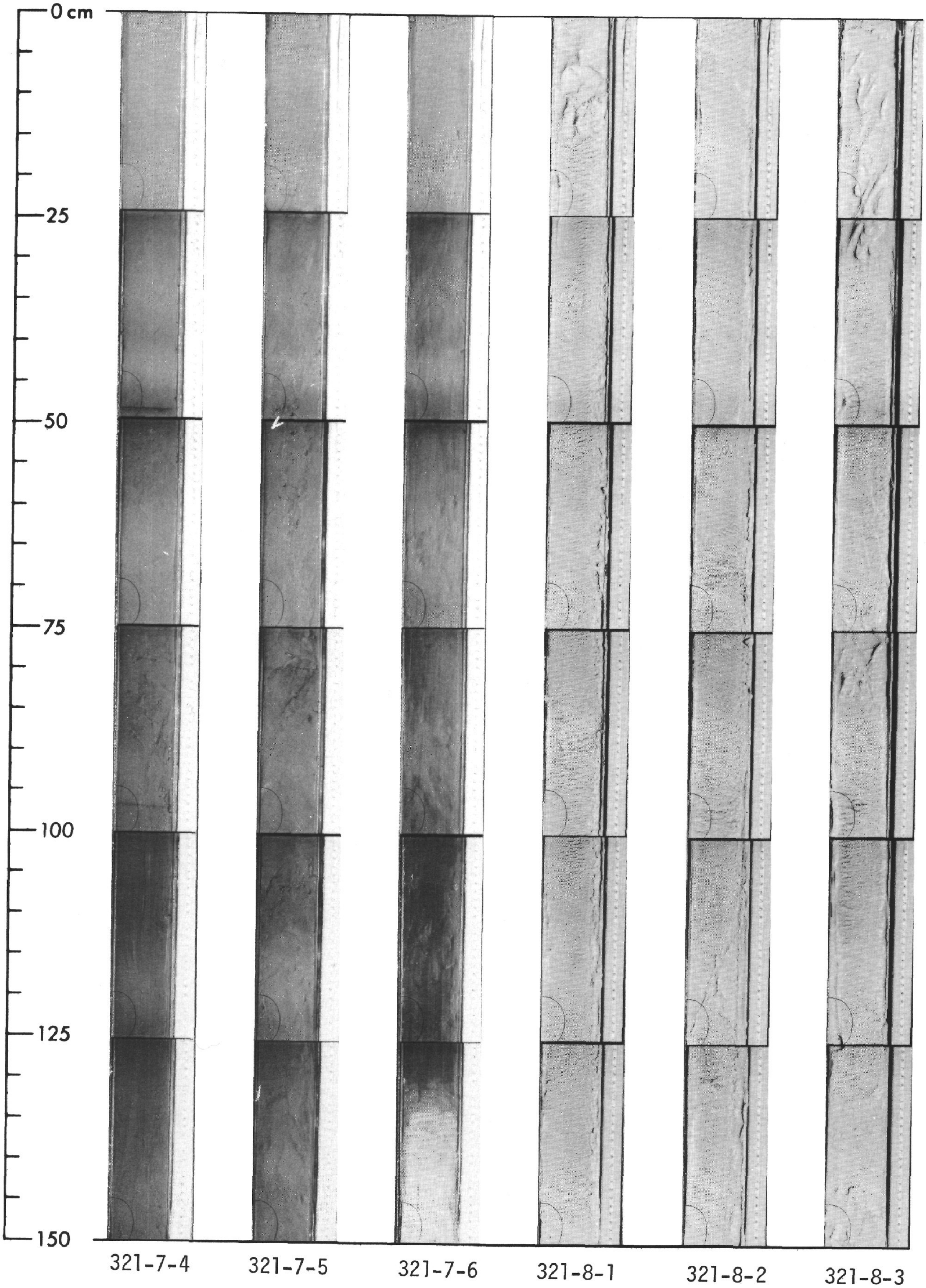
0 cm
25
50
75
100
125
150
321-7-4
321-7-5
321-7-6
321-8-1
321-8-2
321-8-3

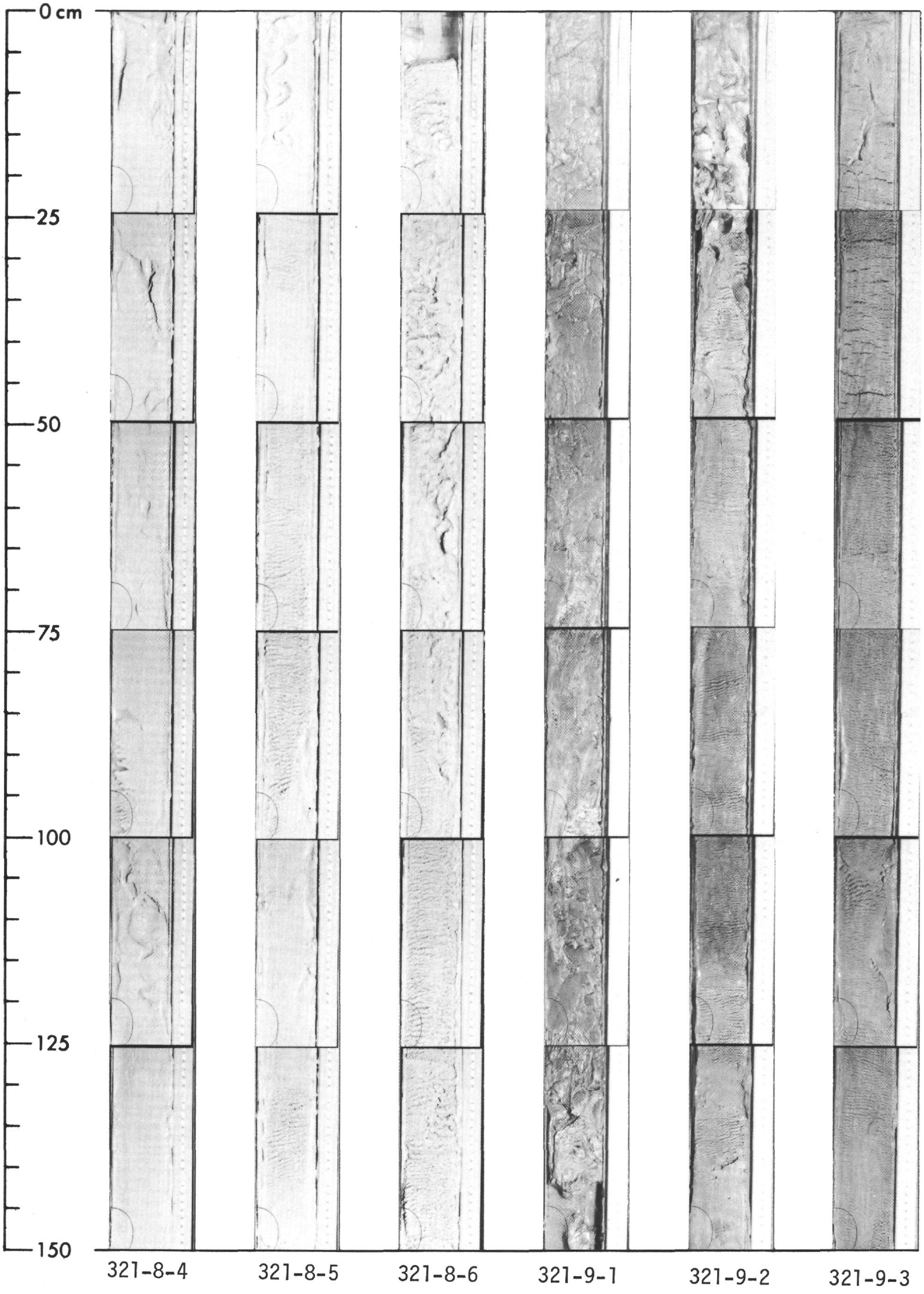
0 cm
25
50
75
100
125
150
321-8-4
321-8-5
321-8-6
321-9-1
321-9-2
321-9-3

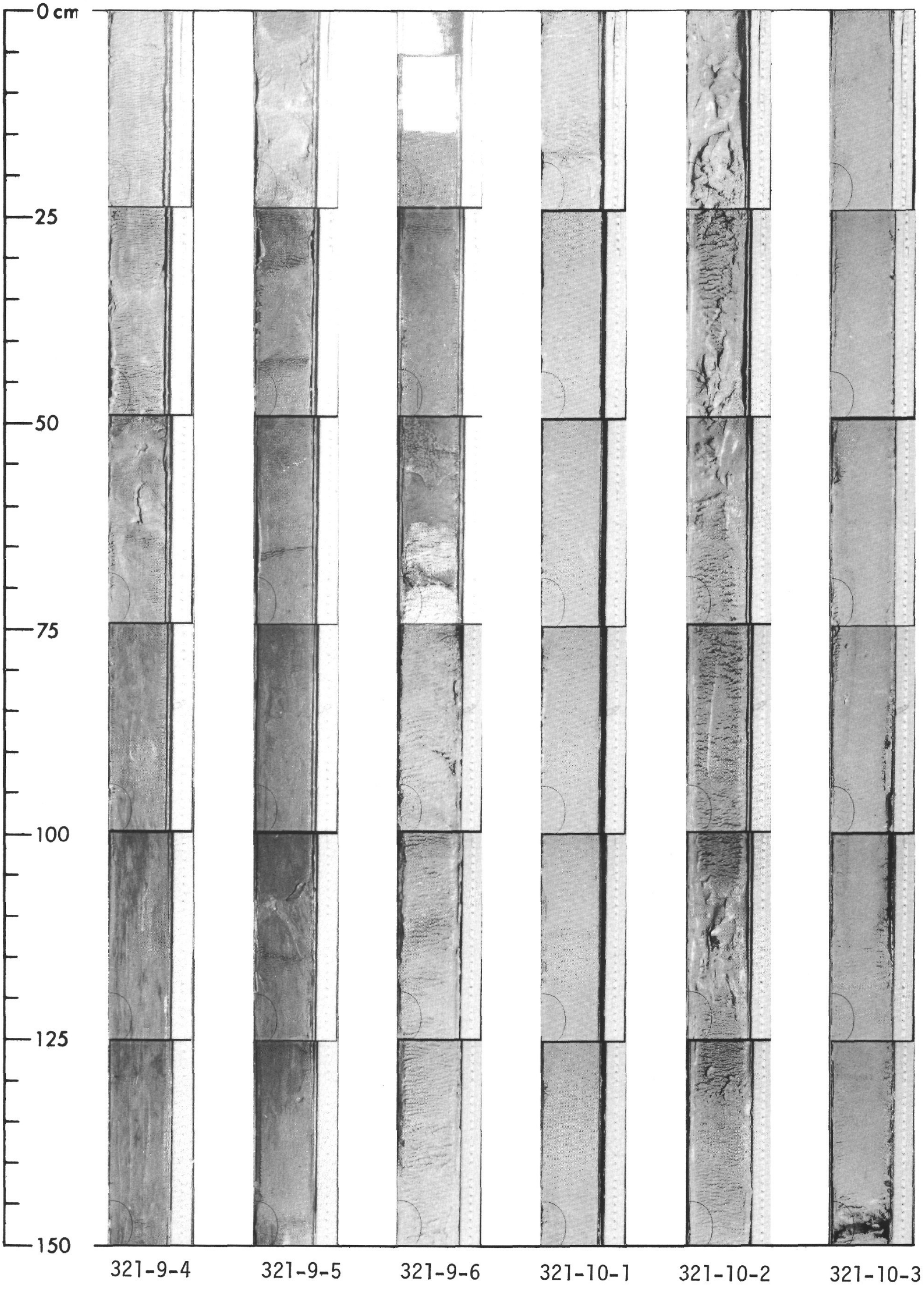
0 cm
25
50
75
100
125
150
321-9-4
321-9-5
321-9-6
321-10-1
321-10-2
321-10-3

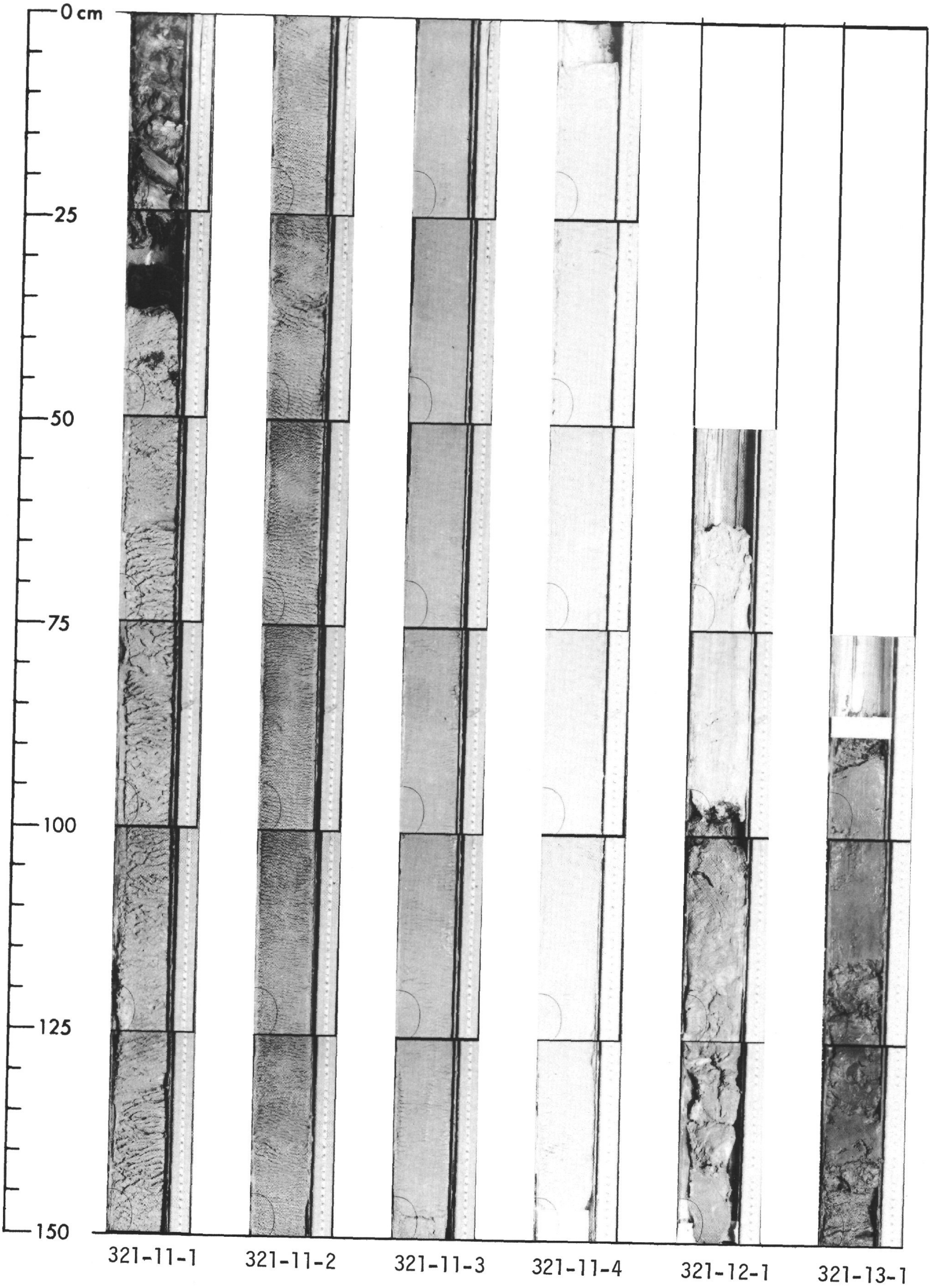

0 cm
25
50
75
100
125
150
321-11-1
321-11-2
321-11-3
321-11-4
321-12-1
321-13-1

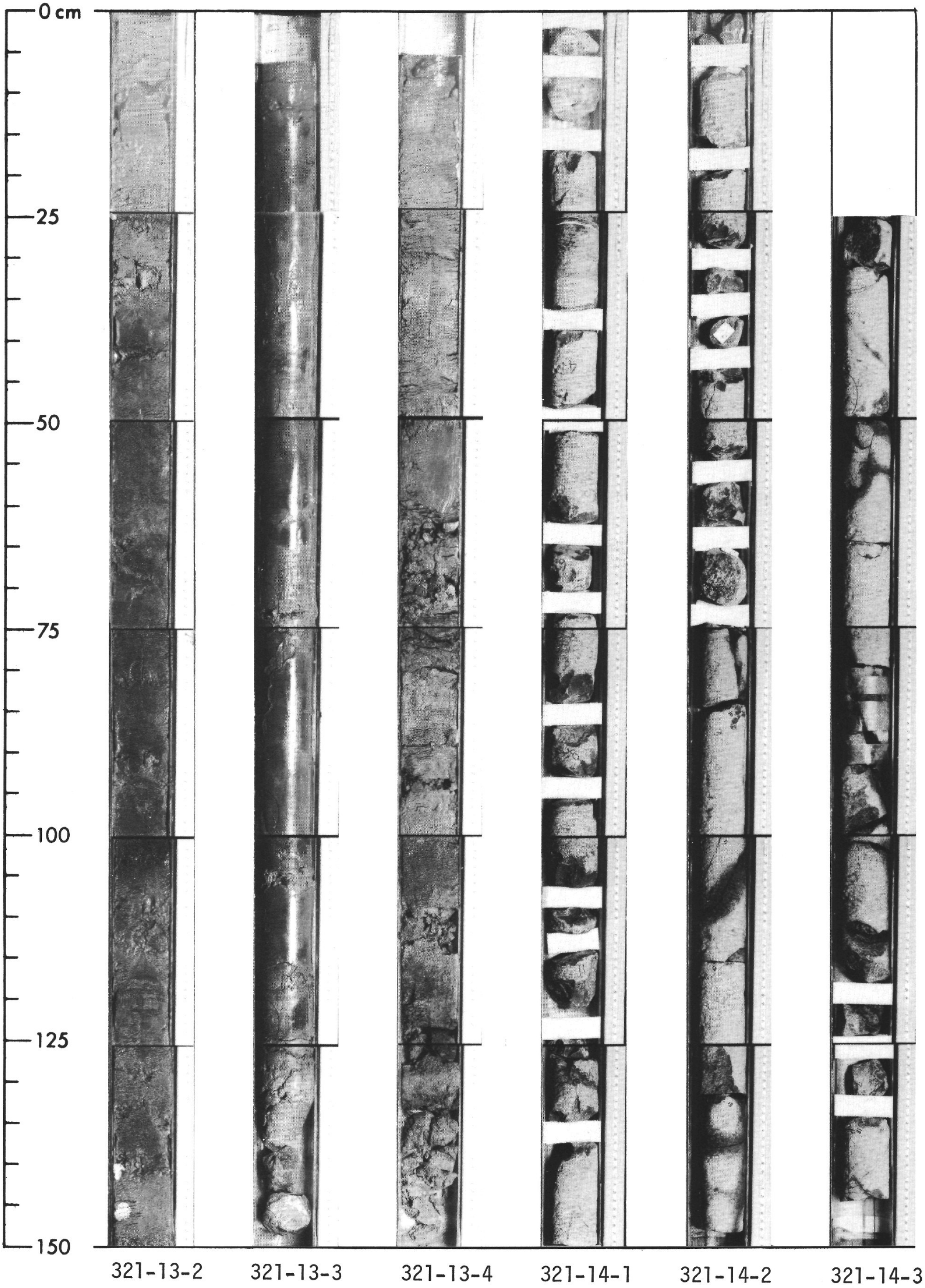
0 cm
25
50
75
100
125
150
321-13-2
321-13-3
321-13-4
321-14-1
321-14-2
321-14-3

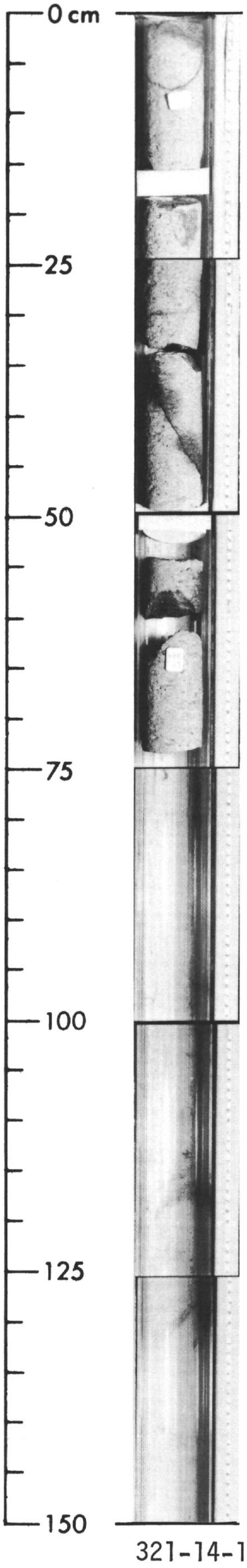
0 cm
25
50
75
100
125
150
321-14-1

Site 321 Hole Core 13 Section 4

Centimeters from Top of Section | Piece Number | Graphic Representation | Section Photograph | Thin Sections | Special Areas | Description

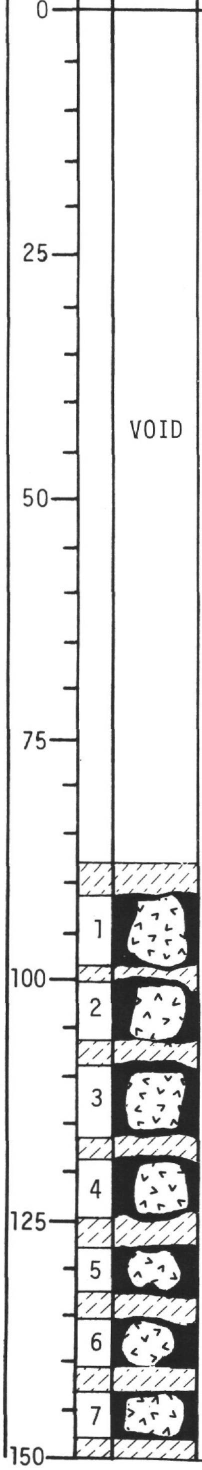

NO PHOTOGRAPH AVAILABLE

Styrofoam spacers, each about 2 cm wide, separate pieces of core that are not part of a continuous core segment. An unknown amount of basalt is missing from the places where the styrofoam has been added.

Fine-grained, light to medium gray or brownish gray, generally unoriented, joint-bounded blocks with outer, relatively altered rims of medium brown or dark brownish to yellowish gray. Aphyric (less than 0.2 mm grain size) except for 2 plagioclases (0.8 x 0.5 and 0.4 x 0.1 mm) and 1 olivine (Ny slightly greater than 1.6784, Fo_{87-88}) in interval 89-98 cm.

0.5% or fewer vesicles up to 0.7 mm diameter (rare larger holes up to 1.1 mm). Generally they are empty in fresher interiors or rarely have blue smectite lining. The outer rims are filled or lined by brown or yellow-green smectite, or stained by Fe-oxide.

Many bounding joints remain where not abraded during drilling. Interior joints are few and nonpenetrative; all other joints were broken during drilling.

Veins of Fe-oxide, Mn-oxide, and brown, brown-green, red-brown, yellow and yellow-green smectite. In 119 to 124 cm, piece 4, a relatively fresh, medium gray, almost unjointed piece, the veins are tan, cream, yellow-green, brown-green and blue smectite.

fragments

Site 321 Hole Core 14 Section 1

Centimeters from Top of Section	Piece Number	Graphic Representation	Section Photograph	Thin Sections	Special Areas	Description

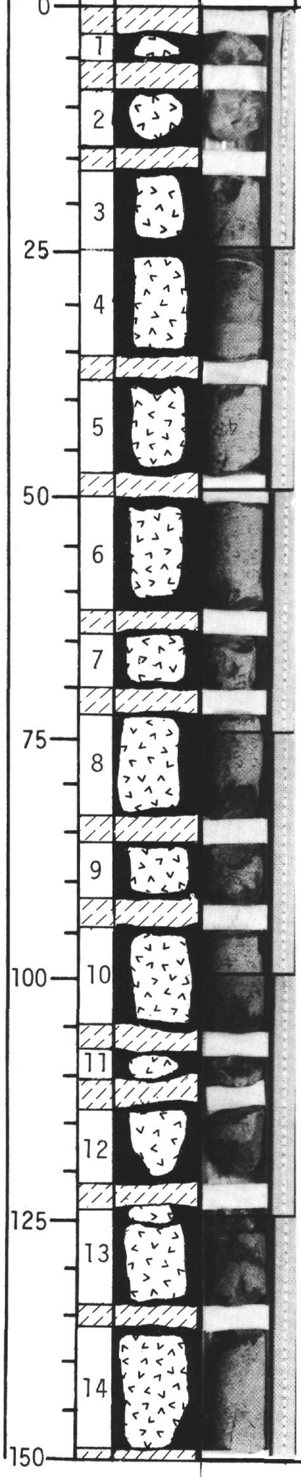

Styrofoam spacers, each about 2 cm wide, separate pieces of core that are not part of a continuous core segment. An unknown amount of basalt is missing from the places where the styrofoam has been added.

Dark gray, fine- to very fine-grained, massive basalt. Coarsens very slightly downward near the top. Apparent decrease in grain size near 86 cm (piece 8) and 113 cm (piece 11); these reversals of the normal increase of grain size downward correspond to the appearance of the only microphenocrysts observed (3 plagioclases and a glomerocryst in pieces 8 and 9, 86 to 105 cm; 2 plagioclases in piece 11, 113 to 121 cm). Otherwise the rocks are aphyric. The changes suggest two contacts separating 3 cooling units.

The top of the section is altered, with marked changes of color in pieces 1 through 3. Green-gray rock occurs in 34 to 40 cm. Dark gray or pinkish gray rock occurs in 40 to 43 cm. Below 43 cm the rock is uniformly gray; no alteration, zoned or otherwise, appears except in veins in piece 8 (86 to 92 cm) and piece 12 (124 to 133 cm).

Fractures bound the surfaces of most core pieces, but internal fractures are absent or nonpenetrative. Vesicles (0.5% to 2%, generally 1%) are present throughout, with maximum sizes less than 1.0 mm, except rarely up to 1.5 mm in 39 to 48 cm; the maximum size is slightly smaller (0.6 to 0.8 mm) in the upper part, above 36 cm. Rare sulfide crystals in carbonate amygdules occur in piece 9 (95 to 105 cm). Near smectite and sulfide veins the amygdules tend to be filled by the vein mineral. The smectite-filled amygdules may be color zoned, and incomplete fillings may have botryoidal inner surfaces.

Veins are composed of smectite, calcite, aragonite, phillipsite and sulfide. Down to 36 cm the smectites are brown, red-brown, and tan, except in 34 to 43 cm where some veins are bright green. Below 36 cm the smectites are blue, blue-green, blue-gray, gray, gray-green, greenish gray, green, yellowish green and black. In 86 to 92 and 124 to 133 cm (pieces 8 and 12) the veins are locally oxidized to yellow-brown and brown. Phillipsite appears in 39 to 48 cm (piece 4) and is last seen in 86 to 92 (piece 8); it is never abundant and appears to be vuggy in some cases. The sulfide first appears at about 42 cm and persists throughout the rest of the section as a major or minor vein component.

Site 321 Hole Core 14 Section 2

Centimeters from Top of Section

Piece Number

Graphic Representation

Section Photograph

Thin Sections

Special Areas

Description

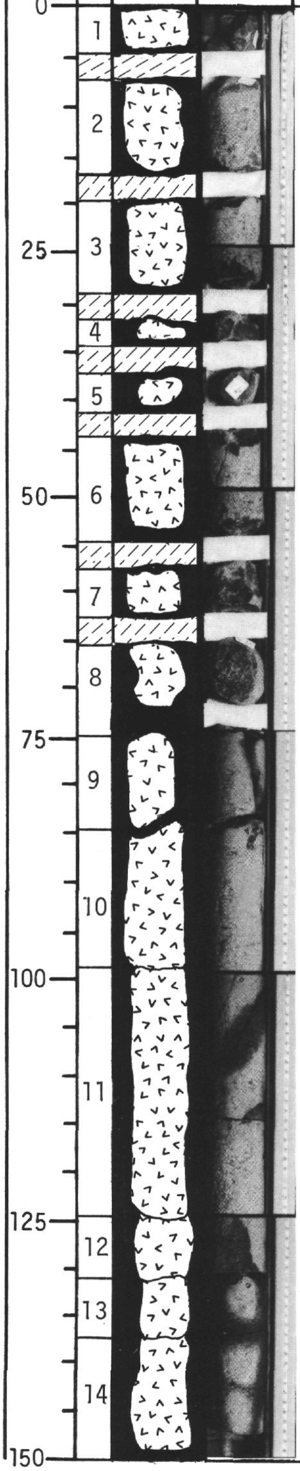

Styrofoam spacers, each about 2 cm wide, separate pieces of core that are not part of a continuous core segment. An unknown amount of basalt is missing from the places where the styrofoam has been added.

Very fine- to medium-grained (mainly fine-grained), dark gray, virtually aphyric basalt. Decrease of grain size at 19 cm correlates with the appearance of rare plagioclase microphenocrysts (1 crystal seen, 1 x 0.3 mm), and may mark the top of a cooling unit. Below that there is a slight coarsening with depth.

Gently to steeply dipping veins are scattered through the top of the section. From 56 to 150 cm, one dominant vertical to steep, branching system of veins is present.

Vesicles vary from a trace to 1.5%, and are generally 0.5% to 1%. Maximum sizes vary from 0.6 to 1.2 mm, and increase in a crude way with depth. Small diktytaxitic vugs are present in piece 3 (19 to 29 cm, the top of the inferred lower cooling unit); they are the only ones seen in basalts from Site 321. Most vesicles are partly or wholly filled by carbonate except near smectite veins (as in piece 3, 19 to 29 cm, piece 5, 37 to 41 cm, and piece 6, 42 to 54 cm) where the vesicles are lined or filled by smectite like that in the veins. In the intermediate zone smectite-lined vesicles may have vuggy, terminated carbonate crystals on their walls. Apparently, empty vesicles appear to be due almost wholly to plucking of smectite or carbonate amygdules during coring.

Veins are mainly smectite -- green, blue-green, blue, dark gray, and gray-green. Sulfides occur in the smectite or form the major component of other veins. Vein carbonate is mainly calcite, in some cases drusy, but includes some aragonite in piece 6 (42 to 54 cm); in general, carbonate is minor in veins. In pieces 3 (19 to 29 cm) and 6 some smectite is locally oxidized brown, red or red-brown along the centers of some veins. In general, though, the veins were tight and oxidizing fluids did not penetrate the interiors of the flow units.

Site 321 Hole Core 14 Section 3

Centimeters from Top of Section	Piece Number	Graphic Representation	Section Photograph	Thin Sections	Special Areas	Description

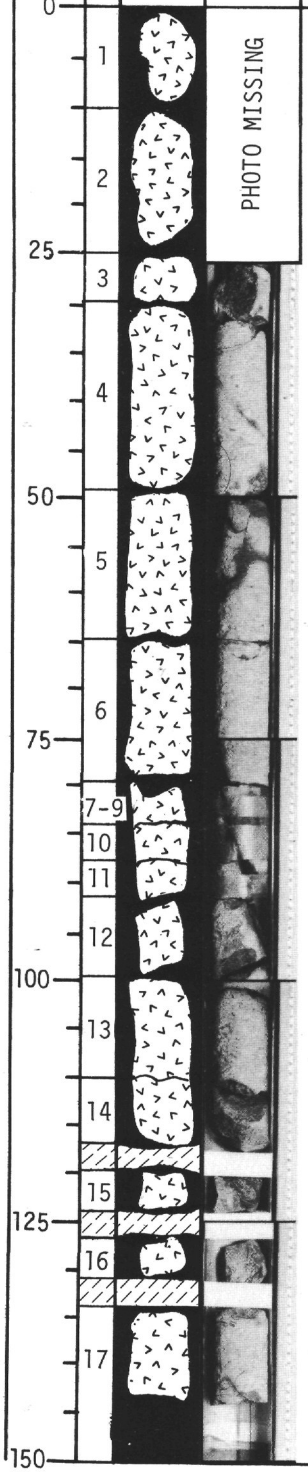

Styrofoam spacers, each about 2 cm wide, separate pieces of core that are not part of a continuous core segment. An unknown amount of basalt is missing from the places where the styrofoam has been added.

Continuous core from 0 to 119 cm of medium- to very coarse-grained, dark gray, aphyric basalt. It coarsens downward. Vesicles are up to 1.3 mm in diameter and form clusters 4 mm across. Down to 119 cm carbonate fillings are common. Below 119 cm they decrease in abundance relative to smectite fillings, and this decrease accompanies a general decrease in abundance of vesicles and amygdules of all sorts to trace amounts at the bottom of the section. Near the top, carbonate amygdules are notably less common near smectite veins than farther away, but through most of the section they occur everywhere, near and far from veins. Other vesicles are smectite-lined or -filled, especially near smectite veins. The smectite is light blue in amygdules in pieces 6 (65 to 80 cm) and 11 (92 to 100 cm). The decrease in vesicle abundance downward in Section 3 emphasizes the local maximum of 1.5% seen in 115 to 131 cm of Section 2, which is the maximum concentration seen in the cooling unit, the top of which occurs at 19 cm in Section 2. The reversal in vesicle frequency below that maximum suggests that the lower contact is approached in Sections 3 and 4, but apparently never quite reach it.

Smectite veins are abundant and of various orientations. They are thick (up to 1.5 mm near the top, thicker below) and tend to swell and cause the core to break up. The main colors of the smectite are gray-green, blue-green, dark gray and green. The blue-green smectite tends to be botryoidal, as it has been throughout Core 14. Scattered sulfide crystals and patches occur in minor amount in the upper part of the section and decrease downward. A calcite vein at 111 cm dips 10°. Below 126 there are thick zoned veins up to 5 or 6 mm thick composed of light tan layers of radial carbonate sandwiched between green smectite zones; locally there may be a total of 3, 5 or 7 layers (i.e., 1, 2 or 3 carbonate layers).

Site 321 Hole Core 14 Section 4

Centimeters from Top of Section	Piece Number	Graphic Representation	Section Photograph	Thin Sections	Special Areas	Description

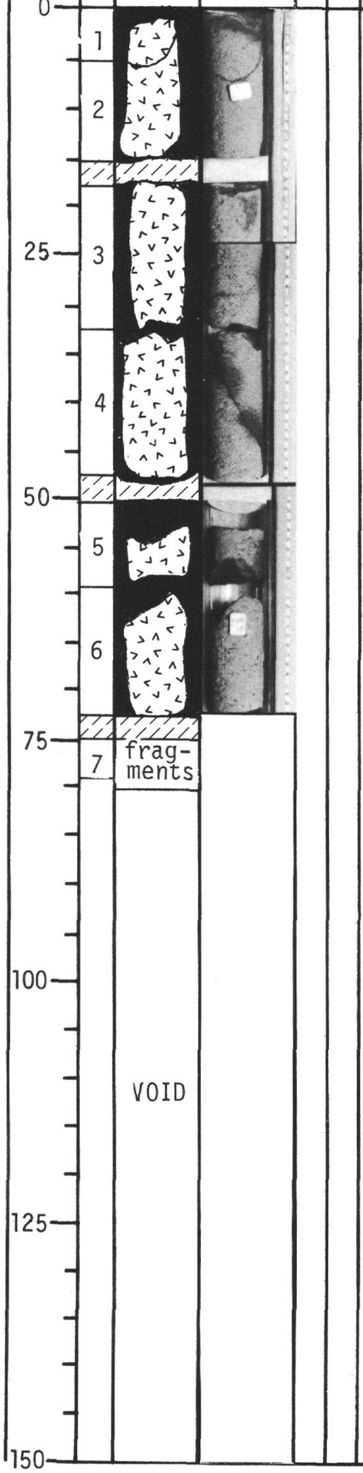

Styrofoam spacers, each about 2 cm wide, separate pieces of core that are not part of a continuous core segment. An unknown amount of basalt is missing from the places where the styrofoam has been added.

Very coarse-grained, dark or medium gray basalt, either aphyric or with at most a trace of phenocrysts. Eight plagioclase microphenocrysts in piece 4 (34 to 49 cm) are up to 1.8 x 0.7 mm and may be locally clustered. Their cores are An_{65-72} (Tsuboi method). In pieces 5 and 6 (51 to 67 cm) there are 10 visibly large crystals ranging in size from 0.6 x 0.2 to 2.4 x 0.6 and 3 x 0.2 mm.

This Section is much less fractured than those above; most veins are steep and those in piece 6 die out within the core; this was not observed higher in the core, where all veins were penetrative, and may mark an approach to a cooling unit contact.

Vesicles in the interval 2 to 16 cm are more abundant (1 to 1.5%) than in the base of Section 3, and may mark a second maximum in this cooling unit (the other being in the interval 115 to 131 cm of Section 2). The maximum size of the vesicles is 1.6 mm. Below 16 cm the abundance of vesicles drops to 0.5%. A few carbonate-filled vesicles occur in 2 to 34 cm, and they may be locally concentrated in certain areas, but the general decrease observed in Section 3 continues, and carbonate amygdules are not seen from 34 to 67 cm.

Veins in 2 to 16 cm are flat to steep, zoned smectite-carbonate veins like those in the lower part of Section 3, but with the addition of light blue spots inside the veins that resemble the light blue amygdules in the host rock (and may be continuous with wall rock amygdules that intersect the vein wall). The main vein component is dark gray-green smectite. Vein sulfide is present as traces at the top of the section. None was seen in the bottom.